

# Coarsening of Disordered Quantum Rotors under a Bias Voltage

Camille Aron\*, Giulio Biroli<sup>†</sup> and Leticia F. Cugliandolo\*

\*Laboratoire de Physique Théorique et Hautes Énergies,

Université Pierre et Marie Curie - Paris VI,

4 Place Jussieu, Tour 13, 5ème étage, 75252 Paris Cedex 05, France.

<sup>†</sup>Institut de Physique Théorique, CEA Saclay, 91191 Gif-sur-Yvette, France.

## Abstract

We solve the dynamics of an ensemble of interacting rotors coupled to two leads at different chemical potential letting a current flow through the system and driving it out of equilibrium. We show that at low temperature the coarsening phase persists under the voltage drop up to a critical value of the applied potential that depends on the characteristics of the electron reservoirs. We discuss the properties of the critical surface in the temperature, voltage, strength of quantum fluctuations, and coupling to the bath phase diagram. We analyze the coarsening regime finding, in particular, which features are essentially quantum mechanical and which are basically classical in nature. We demonstrate that the system evolves via the growth of a coherence length with the same time dependence as in the classical limit,  $R(t) \simeq t^{1/2}$  – the scalar curvature driven universality class. We obtain the scaling function of the correlation function at late epochs in the coarsening regime and we prove that it coincides with the classical one once a prefactor that encodes the dependence on all the parameters is factorized. We derive a generic formula for the current flowing through the system and we show that, for this model, it rapidly approaches a constant that we compute.

# Contents

<b>1</b>	<b>Introduction</b>	<b>4</b>
<b>2</b>	<b>The model</b>	<b>5</b>
2.1	System of disordered quantum rotors . . . . .	5
2.2	Reservoirs of electrons . . . . .	6
2.2.1	DOS with a finite bandwidth . . . . .	7
2.2.2	DOS at low energy . . . . .	8
2.3	Coupling between the system and the reservoirs . . . . .	8
<b>3</b>	<b>The dynamics</b>	<b>9</b>
3.1	Quench setup . . . . .	9
3.2	Schwinger-Keldysh formalism . . . . .	10
3.3	Macroscopic observables . . . . .	11
3.3.1	Keldysh Green's functions . . . . .	12
3.3.2	Self correlation . . . . .	12
3.3.3	Self linear response . . . . .	13
3.3.4	Keldysh rotation . . . . .	13
3.3.5	Bosonic FDT . . . . .	14
<b>4</b>	<b>The influence of the fermion baths</b>	<b>14</b>
4.1	Self-energy . . . . .	14
4.2	Some limits . . . . .	15
4.2.1	Zero drive . . . . .	15
4.2.2	Low frequency . . . . .	16
4.2.3	$\epsilon_F$ much larger than all other energy scales . . . . .	16
4.2.4	Zero temperature . . . . .	17
4.2.5	Some specific reservoirs . . . . .	18
<b>5</b>	<b>Results</b>	<b>18</b>
5.1	Average over disorder . . . . .	19
5.2	Schwinger-Dyson equations . . . . .	20
5.3	Quantum non-equilibrium steady state (QNESS) phase . . . . .	21
5.4	Critical manifold . . . . .	21
5.4.1	Equation for criticality . . . . .	21
5.4.2	Critical points on the $\Gamma = 0$ plane . . . . .	23
5.4.3	Quantum critical point . . . . .	25
5.4.4	Summary of the phase diagram . . . . .	26
5.5	Coarsening phase . . . . .	26
5.5.1	Numerical solution . . . . .	26
5.5.2	Mapping to Langevin dynamics . . . . .	27
5.5.3	Long-time dynamics . . . . .	29
5.5.4	Linear response . . . . .	33
5.5.5	The Lagrange multiplier . . . . .	33

<b>6</b>	<b>The current</b>	<b>35</b>
<b>7</b>	<b>Conclusions and discussion</b>	<b>38</b>
<b>8</b>	<b>Acknowledgments</b>	<b>38</b>
<b>A</b>	<b>Conventions</b>	<b>39</b>
A.1	Fourier transform . . . . .	39
A.2	Heisenberg representation . . . . .	39
A.3	Time-ordering operator . . . . .	40
A.4	Green's functions . . . . .	40
<b>B</b>	<b>Fermionic bath</b>	<b>41</b>
B.1	Keldysh rotation . . . . .	41
B.2	Symmetry properties under $t \leftrightarrow t'$ . . . . .	41
B.3	Free fermions . . . . .	42
B.3.1	Single free fermion . . . . .	42
B.3.2	Collection of free fermions . . . . .	42
B.3.3	Fourier transforms . . . . .	43
<b>C</b>	<b>Fluctuation-Dissipation Theorem</b>	<b>43</b>
<b>D</b>	<b>Computing the self-energy</b>	<b>44</b>
D.1	Derivation within the Schwinger-Keldysh formalism . . . . .	44
D.2	FDT check . . . . .	47
<b>E</b>	<b>Dynamics</b>	<b>48</b>
E.1	Quadratic effective action . . . . .	48
E.2	Saddle-point evaluation . . . . .	49
E.3	Schwinger-Dyson equations . . . . .	50

# 1 Introduction

Quantum mechanics determines the behavior of physical systems at atomic and subatomic scales. The search for quantum effects at macroscopic scales started soon after the development of quantum mechanics. A number of quantum manifestations at such scales have been found including quantum tunneling of the phase in Josephson junctions [1] or resonant tunneling of magnetization in spin cluster systems [2].

Dynamic issues in isolated quantum many-body systems are the focus of active research. Some of the problems that are currently being studied theoretically are: the time evolution of the entropy of entanglement in spin systems [3], the nature of non-equilibrium steady states in small quantum systems driven out of equilibrium [4, 5] due to their relevance for nano-devices, quantum annealing techniques [6], and the density of defects left over after a gradual change in a parameter [7]. The influence of an environment on the dynamics of quantum systems was also dealt with in a number of cases such as the spin-boson model [1], disordered spin chains coupled to bosonic baths [8], or an electronic ring coupled to leads and further driven by a time-dependent field [9, 10].

Once the interest is set upon macroscopic systems, the question as to whether these undergo phase transitions naturally arises. The theory of equilibrium classical and quantum phase transitions is well developed. *Non-equilibrium* phase transitions in which quantum fluctuations can be neglected are also quite well understood. These are realized when a system is forced in a non equilibrium steady state (by a shear rate, an external current flowing through it, etc.) [11, 12, 13, 14] or when it just fails to relax (*e.g.* after a quench) and displays aging phenomena [15, 16]. In contrast, the effect of a drive on a *macroscopic* system close to a quantum phase transition is a rather unexplored subject. Some works have focused on non-linear transport properties close to an (equilibrium) quantum phase transition [17, 18, 19]. Others have studied how the critical properties are affected by non-equilibrium drives [20, 21, 22]. However, a global understanding of phase transitions in the control parameter space  $T, V, \Gamma$ , with  $T$  the temperature,  $V$  the driving strength, and  $\Gamma$  the strength of quantum fluctuations, is still lacking. Furthermore, to the best of our knowledge, the issue of the *relaxation* toward the quantum non-equilibrium steady state (QNESS) has not been addressed in the past.

In this paper we extend our study of driven quantum phase transitions and coarsening phenomena started in [23]. We study a class of analytically tractable models, systems of  $M$ -component  $N$  quantum rotors that encompass an infinite range spin-glass and its three dimensional pure counterpart modeling coarsening phenomena. As discussed in [24] models of quantum rotors are non-trivial but still relatively simple and provide coarse-grained descriptions of physical systems such as Bose-Hubbard models and double layer antiferromagnets. The system is coupled to two different external electron reservoirs that lead to a current flowing through it and driving it out of equilibrium. (For a two-dimensional model the current flows perpendicular to it, see the sketch in Fig. 1 of [20].) In the simplest setting [20] each rotor is coupled to independent reservoirs; more realistic couplings are discussed in [22]. Using the Schwinger-Keldysh formalism [25, 26] we obtain the complete out of equilibrium dynamics of these models in the large  $M$  limit. We show that at sufficiently low  $T, V, \Gamma$ , see Fig. 1, the system never reaches a QNESS and ages with remarkable universal properties. We study the critical properties of the phase transitions, in particular in the vicinity of the (drive-induced)

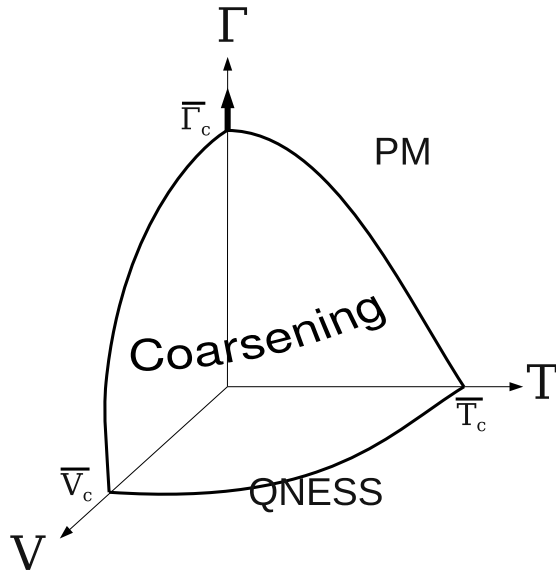


Figure 1: Non-equilibrium phase diagram of the fully connected driven quantum rotor model with an infinite number of components.

quantum out of equilibrium critical point  $\bar{V}_c$  at  $\Gamma = 0, T = 0$  and the “usual” quantum critical point  $\bar{\Gamma}_c$  at  $V = 0, T = 0$ . We analyze in detail the relaxation in the coarsening regime and uncover the scaling properties of correlation functions and linear response. We derive a general formula for the current flowing through the system under such a voltage drop and we analyze its dependence on the dynamics of the system. Some of these results were announced recently in [23].

## 2 The model

### 2.1 System of disordered quantum rotors

The model we focus on is a quantum disordered system made of  $N$   $M$ -component rotors interacting via random infinite-range couplings [27]. We consider a fully-connected (mean-field) model where there is no underlying geometry: each rotor is equivalently coupled to all the others. The Hamiltonian is given by

$$H_S = \frac{\Gamma}{2M} \sum_{i=1}^N \mathbf{L}_i^2 - \frac{M}{\sqrt{N}} \sum_{i,j < i} J_{ij} \mathbf{n}_i \cdot \mathbf{n}_j . \quad (2.1)$$

$n_i^\mu$  ( $\mu = 1 \dots M$ ) are the  $M$  components of the  $i$ -th rotor. The coordinates  $n_i^\mu$  constitute a complete set of commuting observables. The scalar product  $\mathbf{n}_i \cdot \mathbf{n}_j$  is given by  $\sum_{\mu=1}^M n_i^\mu n_j^\mu$ . The length of rotors is fixed to unity:  $\mathbf{n}_i \cdot \mathbf{n}_i = 1, \forall i = 1 \dots N$ . The strengths  $J_{ij}$ ’s are taken from a Gaussian distribution with zero mean and variance  $J^2$ .  $J$  controls the strength of disorder.  $\mathbf{L}_i$

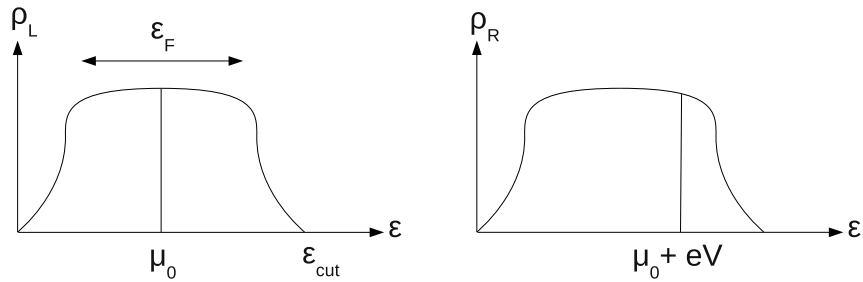


Figure 2: Density of states (DOS) of type A reservoirs.  $\mu_0$  and  $\mu_0 + eV$  are the left and right Fermi levels, respectively. The left reservoir is half-filled.

is the  $i$ -th generalized angular momentum operator which  $M(M - 1)/2$  components are given by

$$L_i^{\mu\nu} = -i\hbar \left( n_i^\mu \frac{\partial}{\partial n_i^\nu} - n_i^\nu \frac{\partial}{\partial n_i^\mu} \right) \quad \text{for } 1 \leq \mu < \nu \leq M, \quad (2.2)$$

$$\mathbf{L}_i^2 = \sum_{\mu < \nu} (L_i^{\mu\nu})^2 \quad [24, 27].$$

$\Gamma$  acts like a moment of inertia and controls the strength of quantum fluctuations; when  $\hbar^2\Gamma/J \rightarrow 0$  the model approaches the classical Heisenberg fully-connected spin-glass. In the large  $M$  limit it is equivalent to the quantum fully-connected  $p = 2$  (or Sherrington-Kirkpatrick) spherical spin-glass [28, 29]. The classical mapping to ferromagnetic coarsening in the  $O(\mathcal{N})$  model with  $\mathcal{N} \rightarrow \infty$  [16] holds, as we shall show in Sect. 5.5.3, for the quantum model as well.

## 2.2 Reservoirs of electrons

The system is coupled to two, ‘left’ ( $L$ ) and ‘right’ ( $R$ ), reservoirs of electrons. These independent reservoirs are both in equilibrium at inverse temperature  $\beta_L$  and  $\beta_R$ . The situation  $\beta_L \neq \beta_R$  would create a heat flow from one reservoir to the other. We are interested in the simpler case in which  $\beta_L = \beta_R \equiv \beta \equiv T^{-1}$  ( $k_B = 1$ ). An electric current is forced by imposing different chemical potentials,  $\mu_L = \mu_0$  and  $\mu_R = \mu_0 + eV$  (where  $-e$  is the electric charge of one electron).  $eV$  is the strength of the drive. As  $eV/J \rightarrow 0$ , the effect of the reservoirs on the system approaches the one of an equilibrium bath at temperature  $T$ . The details of the reservoir Hamiltonians  $H_L$  and  $H_R$  are not important since only the electronic Green’s functions matter in the small rotor-bath coupling we concentrate on. We consider the simple case in which left and right fermionic reservoirs have the same density of states (DOS)  $\rho_L = \rho_R = \rho$ . Moreover, we focus on simple cases in which the shape of the DOS is controlled by only one typical energy scale  $\epsilon_F$ . In the rest of this paper, we often consider the limit in which  $\epsilon_F$  is much larger than all the other energy scales involved. In this limit the results become independent of the detailed functional form of the DOS. We also give some results for finite  $\epsilon_F$  using the specific DOS that we introduce below.

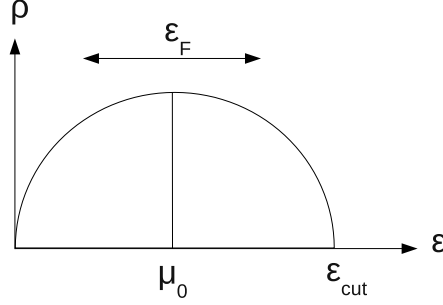


Figure 3: An example of type A reservoir: the semi-circle density of states (half-filled).

### 2.2.1 DOS with a finite bandwidth

We first consider regular DOS which have a finite typical width (finite bandwidth) controlled by  $\epsilon_F$  and  $\mu_0$  is set around the maximum of the distribution. In the limit where  $\epsilon_F$  is very large, they can be seen as almost flat distributions. We call  $\epsilon_{cut}$  the finite energy cut-off beyond which the DOS vanishes,  $\rho(|\epsilon| > \epsilon_{cut}) = 0$ . Since the DOS we consider have a single energy scale  $\epsilon_F$ ,  $\epsilon_{cut}$  should scale with  $\epsilon_F$ . Notice that a finite  $\epsilon_{cut}$  constrains the voltage not to exceed  $eV_{max} = \epsilon_{cut} - \mu_0$  since the right reservoir is then completely filled and therefore it cannot accept more fermions.

We call reservoir of type A a half-filled<sup>1</sup> reservoir the DOS of which has a finite bandwidth controlled by  $\epsilon_F$  and is symmetric and derivable in the vicinity of its maximum (see Fig. 2). The simplest example of a type A reservoir is given by the semi-circular DOS (see Fig. 3),

$$\rho_A(\epsilon) \equiv \frac{2}{\pi\epsilon_F} \sqrt{1 - \left(\frac{\epsilon - \epsilon_F}{\epsilon_F}\right)^2}, \quad (2.3)$$

that is symmetric and centered around  $\epsilon_F$ . Here  $\epsilon_{cut} = 2\epsilon_F$ . We choose  $\mu_0 = \epsilon_F$  so that the reservoirs are half-filled at zero drive ( $eV = 0$ ). In this case, at  $T = 0$ , the voltage applied between both reservoirs cannot exceed  $eV_{max} = \epsilon_{cut} - \mu_0 = \epsilon_F$ .

Type B reservoirs have finite bandwidth but no energy cut-off:  $\epsilon_{cut} = eV_{max} \rightarrow \infty$ . A realization of these reservoirs is given by the following DOS [see Fig. 4(a)]

$$\rho_B(\epsilon) \equiv \frac{\alpha}{\epsilon_F} \sqrt{\frac{\epsilon}{\epsilon_F}} e^{-\frac{1}{2}\left(\frac{\epsilon}{\epsilon_F}\right)^2}, \quad (2.4)$$

where  $\alpha \approx 0.97$  is a numerical constant fixed by normalization. The maximum of this distribution is located at  $\epsilon_F/\sqrt{2}$ . This reservoir is half-filled for  $\mu_0 \approx 0.95 \epsilon_F$ . This distribution resembles the semi-circular one in the sense that they both start with a square root behavior, have a maximum, and a bandwidth of order  $\epsilon_F$ . In contrast, the DOS in eq. (2.4) is different from zero at all finite  $\epsilon$  and one can exploit this feature to apply strong voltages.

<sup>1</sup>Half-filled means that half the total number of available states are occupied:  $\int_{-\infty}^{\mu_0} d\epsilon \rho(\epsilon) = \frac{1}{2}$  at  $T = 0$ .

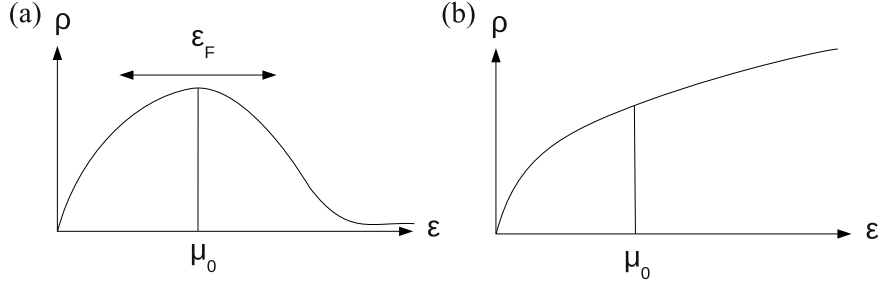


Figure 4: Two examples of type  $B$  reservoirs. (a) The distribution  $\rho_B$  vanishes asymptotically. (b) The square root distribution diverges asymptotically.

### 2.2.2 DOS at low energy

In the previous examples ( $\rho_A$  and  $\rho_B$ ), we focused on values of  $\mu_0$  corresponding to high energy states where the DOS is regular. We are also interested in studying cases where  $\mu_0$  is centered around low energy states. To analyze these cases, we focus on a DOS which reads [see Fig. 4(b)]:

$$\rho_{C3d}(\epsilon) \equiv \frac{3}{4\sqrt{2}\epsilon_F} \sqrt{\frac{\epsilon}{\epsilon_F}}. \quad (2.5)$$

This square root behavior is actually the one of the  $3d$  free fermions reservoir. In this case  $\epsilon_F$  is of the order of the hopping term for the free fermions. Since we shall only focus on the low energy states of the reservoir, we can neglect the non trivial high energy structure of the reservoir and take the DOS equal to zero for  $\epsilon > 2\epsilon_F$ .

For the  $2d$  free fermions, the density of states is given by

$$\rho_{C2d}(\epsilon) \equiv \frac{1}{2\epsilon_F}, \quad (2.6)$$

whereas for the  $1d$  free fermions, the density of states is given by

$$\rho_{C1d}(\epsilon) \equiv \frac{1}{2\sqrt{2}\epsilon_F} \sqrt{\frac{\epsilon_F}{\epsilon}} \quad (2.7)$$

and, as for  $\rho_{C3d}$ , we take these two densities of states to be equal to zero for  $\epsilon > 2\epsilon_F$ .

## 2.3 Coupling between the system and the reservoirs

An electron hop from the  $L(R)$  reservoir to the  $R(L)$  reservoir is linearly coupled to each rotor component:

$$H_{SB} = -\frac{\sqrt{M}}{N_s} \sum_{i=1}^N \sum_{\mu=1}^M \sum_{k,k'=1}^{N_s} \sum_{l,l'=1}^M V_{kk'} n_i^\mu [\psi_{Likl}^\dagger \sigma_{ll'}^\mu \psi_{Rik'l'} + L \leftrightarrow R], \quad (2.8)$$

where  $\psi_{Likl}^\dagger$  is the  $l$ -th component of an  $\mathcal{M}$ -component spinor operator that creates an additional fermion with energy  $\hbar\omega_k$  in the  $L$  reservoir associated to the  $i$ -th rotor.  $k$  labels the electron



energy inside the reservoirs,  $N_s$  is the total number of states in each reservoir.  $\sigma^\mu$  are the generalized Pauli matrices for  $SU(\mathcal{M})$  of dimension  $\mathcal{M} \times \mathcal{M}$  with  $\mathcal{M}^2 - 1 = M$ . They are chosen to be normalized such that  $\text{Tr} \sigma^\mu \sigma^\nu = \delta_{\mu\nu}$ .  $V_{kk'}$  are the rotor-environment coupling parameters chosen to be constant:  $V_{kk'} = \hbar\omega_c$ .  $H_{SB}$  is  $\mathcal{O}(MN)$  invariant.

### 3 The dynamics

#### 3.1 Quench setup

The system is initially prepared (at times  $t < 0$ ) in such a way that its initial configuration (at time  $t = 0$ ) is neither correlated with disorder ( $J_{ij}$ 's) nor with the reservoirs. This can be realized, for instance, by coupling the system to an equilibrium bath at temperature  $T_0 \gg J, \Gamma$  so that any correlation in the system is suppressed. At time  $t = 0$  the quench is performed by suddenly coupling the system to the  $L$  and  $R$  reservoirs. These are supposed to be “good reservoirs” in the sense that their properties are not affected by the state of the system.

This setup generates non-equilibrium dynamics at times  $t > 0$  for multiple reasons. First of all, the rapid quenching procedure puts the system in a non-equilibrium initial condition with respect to its new environment. Moreover, the latter is not an equilibrium bath but a bias drive the role of which is to constantly destabilize the system. Finally, as a consequence of its disordered interactions, the system of rotors experiences intrinsic difficulties to reach equilibrium. Indeed, even if it were embedded within an equilibrium environment it would show a glassy phase [29, 31] in some parts of the phase diagram.

Since system and reservoirs are decoupled at times  $t < 0$ , the initial density matrix of the whole system is given by

$$\varrho(t=0) = \varrho_S(t=0) \otimes_{i=1}^N \varrho_{Li} \otimes_{i=1}^N \varrho_{Ri} . \quad (3.1)$$

$\varrho_{Li/Ri}$  corresponds to the equilibrium density matrix of the  $L/R$  reservoir associated with the  $i$ -th rotor. The system of rotors being prepared at very high temperature, its initial density matrix is the identity in the rotors space:

$$\varrho_S(t=0) \propto I_S . \quad (3.2)$$

All these density matrices are normalized to be of unit trace. The  $t > 0$  evolution of the whole system plus environment is encoded in

$$\varrho(t) = U(t,0) \varrho(0) [U(t,0)]^\dagger , \quad (3.3)$$

where the unitary evolution operator is given by  $U(t,0) \equiv \mathbb{T} e^{-\frac{i}{\hbar} \int_0^t dt' H(t')}$  with  $H = H_S + H_L + H_R + H_{SB}$  and  $\mathbb{T}$  the time-ordering operator (see Appendix A). We analyze the non-equilibrium dynamics using the Schwinger-Keldysh formalism (see [26] for a modern review) that we briefly introduce in the following lines.

### 3.2 Schwinger-Keldysh formalism

The Suzuki-Trotter decomposition of the two unitary evolution operators that appear in

$$\mathcal{Z} \equiv \lim_{\tau \rightarrow \infty} \text{Tr} U(\tau, 0) \varrho(0) [U(\tau, 0)]^\dagger = 1, \quad (3.4)$$

yields a path-integral involving two sets of fields with support on two different branches. The first ones are time-integrated on a forward branch from  $t = 0$  to  $+\infty$ . In the following, these fields carry a  $+$  superscript. The other ones are time-integrated on a backward branch from  $+\infty$  to  $0$  and carry a  $-$  superscript. These two branches constitute the Keldysh contour  $\mathcal{C}$ , see Fig. 5. The identity (3.4) can now be expressed as a path integral,

$$\mathcal{Z} = \int_{\mathcal{C}} \mathcal{D}[\mathbf{n}^\pm, \boldsymbol{\psi}^\pm, \bar{\boldsymbol{\psi}}^\pm] e^{\frac{i}{\hbar} S} \langle \mathbf{n}^+(0), \bar{\boldsymbol{\psi}}^+(0) | \varrho(0) | \mathbf{n}^-(0), \boldsymbol{\psi}^-(0) \rangle, \quad (3.5)$$

where we collected all the  $n_i^{\mu a}$  fields into the notation  $\mathbf{n}^a$ , and all the fermionic fields  $\psi_{\alpha i}^a$  and their Grassmannian conjugates into  $\boldsymbol{\psi}^a$  and  $\bar{\boldsymbol{\psi}}^a$  (with  $a = \pm$ ).  $\langle \mathbf{n}^+(0), \bar{\boldsymbol{\psi}}^+(0) | \varrho(0) | \mathbf{n}^-(0), \boldsymbol{\psi}^-(0) \rangle$  is the matrix element of the density matrix which has support at time  $t = 0$  only. The action  $S$  is a functional of all these fields:

$$S = \sum_{a=\pm} a \int_0^\infty dt \mathcal{L}([\mathbf{n}^a, \boldsymbol{\psi}^a, \bar{\boldsymbol{\psi}}^a]; t). \quad (3.6)$$

The Lagrangian is given by  $\mathcal{L} = \mathcal{L}_S + \mathcal{L}_{SB} + \mathcal{L}_L + \mathcal{L}_R$  with

$$\mathcal{L}_S([\mathbf{n}^a]; t) = \frac{M}{2\Gamma} \sum_i \dot{\mathbf{n}}_i^a(t)^2 + \frac{M}{\sqrt{N}} \sum_{i,j < i} J_{ij} \mathbf{n}_i^a(t) \cdot \mathbf{n}_j^a(t), \quad (3.7)$$

$$\mathcal{L}_{SB}([\mathbf{n}^a, \boldsymbol{\psi}^a, \bar{\boldsymbol{\psi}}^a]; t) = \sqrt{M} \frac{\hbar \omega_c}{N_s} \sum_{i\mu k k' l l'} n_i^{\mu a}(t) [\bar{\boldsymbol{\psi}}_{L i k l}^a(t) \sigma_{l l'}^\mu \boldsymbol{\psi}_{R i k' l'}^a(t) + L \leftrightarrow R]. \quad (3.8)$$

$\mathcal{L}_L$  and  $\mathcal{L}_R$  are the Lagrangians of the free fermions in the  $L$  and  $R$  reservoirs. The index ‘c’ at the bottom of the integral sign in eq. (3.5) is here to remind us that the integration is performed over fields satisfying the constraint that each rotor has a fixed unit length:  $\mathbf{n}_i^a(t)^2 = 1 \forall a, i, t$ . The path-integral formalism gives a nice way to restore an unconstrained integration over all fields  $\mathbf{n}_i^a$  by the introduction of Lagrange multipliers  $z_i^a$ :

$$\int_{\mathcal{C}} \mathcal{D}[\mathbf{n}^a] = \int \mathcal{D}[\mathbf{n}^a] \prod_{i,t} \delta(1 - \mathbf{n}_i^a(t)^2) \quad (3.9)$$

$$= \int \mathcal{D}[\mathbf{n}^a, z^a] \exp \left( \frac{i}{\hbar} \int_0^\infty dt a \frac{M}{2} \sum_i z_i^a(t) (1 - \mathbf{n}_i^a(t)^2) \right). \quad (3.10)$$

where we used the integral representation of the delta function (see Appendix A) and collected the new auxiliary real fields  $z_i^a$  into the notation  $z^a$ . In terms of a Lagrangian, this gives rise to the new term

$$\mathcal{L}_{LM}([\mathbf{n}^a, z^a]; t) = \frac{M}{2} \sum_i z_i^a(t) [1 - \mathbf{n}_i^a(t)^2]. \quad (3.11)$$

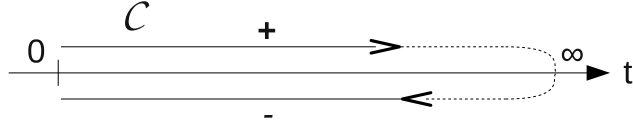


Figure 5: The Keldysh contour  $\mathcal{C}$  goes from 0 to  $+\infty$  and then back to 0. The Keldysh action involves forward fields (that live on the  $+$ -branch of  $\mathcal{C}$ ) that are time-integrated from 0 to  $+\infty$  and backward fields (that live on the  $-$ -branch of  $\mathcal{C}$ ) and are time-integrated from  $+\infty$  to 0.

### 3.3 Macroscopic observables

We are interested in the macroscopic dynamics of the rotors after an infinitely rapid quench and we wish to give an answer to the following questions (among others). Does the system reach a steady state? Does a steady state current establish? What are the long-time dynamics? We first obtain an effective generating functional for the rotors by expanding the system-drive interaction up to second order in the coupling, integrating away the fermionic degrees of freedom, and averaging over the disorder distribution.

Introducing the external real fields  $\eta_{i\mu}^a(t)$  that we collect in the notation  $\boldsymbol{\eta}^a(t)$  ( $a = \pm$ ), the generating functional  $\mathcal{Z}[\boldsymbol{\eta}^\pm]$  reads

$$\mathcal{Z}[\boldsymbol{\eta}^\pm] \equiv \int \mathcal{D}[\mathbf{n}^\pm, z^\pm, \boldsymbol{\psi}^\pm, \bar{\boldsymbol{\psi}}^\pm] e^{\frac{i}{\hbar} S[\mathbf{n}^\pm, z^\pm, \boldsymbol{\psi}^\pm, \bar{\boldsymbol{\psi}}^\pm, \boldsymbol{\eta}^\pm]} \langle \mathbf{n}^+(0), \bar{\boldsymbol{\psi}}^+(0) | \varrho(0) | \mathbf{n}^-(0), \boldsymbol{\psi}^-(0) \rangle, \quad (3.12)$$

where we introduced the source term

$$S \longmapsto S + \hbar \sum_{a=\pm} \int dt \sum_i \sum_\mu n_i^{\mu a}(t) \eta_i^{\mu a}(t). \quad (3.13)$$

The generating functional obeys the normalization property  $\mathcal{Z}[\boldsymbol{\eta}^\pm = \mathbf{0}] = \mathcal{Z} = 1$  which is a fundamental feature of the Keldysh formalism in this setup (see eq. (3.4) and Sect. 5.1). One has

$$\langle n_i^{\mu a}(t) \rangle = -\frac{i}{\mathcal{Z}} \frac{\delta \mathcal{Z}[\boldsymbol{\eta}^\pm]}{\delta \eta_i^{\mu a}(t)} \Big|_{\boldsymbol{\eta}^\pm = \mathbf{0}}, \quad (3.14)$$

where we introduced the notation

$$\langle \dots \rangle \equiv \int \mathcal{D}[\mathbf{n}^\pm, z^\pm, \boldsymbol{\psi}^\pm, \bar{\boldsymbol{\psi}}^\pm] \dots e^{\frac{i}{\hbar} S} \langle \mathbf{n}^+(0), \bar{\boldsymbol{\psi}}^+(0) | \varrho(0) | \mathbf{n}^-(0), \boldsymbol{\psi}^-(0) \rangle. \quad (3.15)$$

Notice that one can distinguish this bracket notation from the quantum statistical average that we denote similarly by the occurrence of Keldysh indices inside the brackets. However, they coincide in the case of one time observables, *e.g.*

$$\langle n_i^\mu(t) \rangle = \langle n_i^{\mu a}(t) \rangle, \quad (3.16)$$

with  $a = +$  or  $-$  equivalently if the observable is time-reversal invariant.

### 3.3.1 Keldysh Green's functions

We introduce the two-time Green's functions  $G_{ij\mu\nu}^{ab}(t, t')$ , defined on the Keldysh contour ( $a, b = \pm$ ), as

$$\langle n_i^{\mu a}(t) n_j^{\nu b}(t') \rangle = -\frac{1}{\mathcal{Z}} \frac{\delta^2 \mathcal{Z}[\boldsymbol{\eta}^\pm]}{\delta \eta_i^{\mu a}(t) \delta \eta_j^{\nu b}(t')} \Big|_{\boldsymbol{\eta}^\pm=0} \equiv i\hbar G_{ij\mu\nu}^{ab}(t, t'). \quad (3.17)$$

$n_i^{\mu a}$  being real fields, one has the following time-reversal property

$$G_{ij\mu\nu}^{ab}(t, t') = G_{jiv\mu}^{ba}(t', t). \quad (3.18)$$

In the operator formalism, the Keldysh Green's functions read

$$i\hbar G_{ij\mu\nu}^{ab}(t, t') = \text{Tr} \left[ \mathbb{T}_C n_{iH}^\mu(t, a) n_{jH}^\nu(t', b) \varrho(0) \right], \quad (3.19)$$

where  $n_{iH}^\mu(t, a)$  denotes the Heisenberg representation of the operator  $n_i^\mu$  at time  $t$  and on the  $a$ -branch of the Keldysh contour.  $\mathbb{T}_C$  is the time-ordering operator acting with respect to the relative position of  $(t, a)$  and  $(t', b)$  on the Keldysh contour  $\mathcal{C}$  (see Appendix A).

We define the macroscopic Keldysh Green's functions by summing over the  $N$  rotors and each of their  $M$  components

$$G^{ab}(t, t') \equiv \frac{1}{N} \sum_{i=1}^N \sum_{\mu=1}^M G_{ii\mu\mu}^{ab}(t, t'). \quad (3.20)$$

From the identity (3.19), one establishes two relations between the four Green's functions

$$\begin{aligned} G^{++}(t, t') &= G^{-+}(t, t')\Theta(t - t') + G^{+-}(t, t')\Theta(t' - t), \\ G^{--}(t, t') &= G^{+-}(t, t')\Theta(t - t') + G^{-+}(t, t')\Theta(t' - t), \end{aligned} \quad (3.21)$$

leading to

$$\begin{aligned} G^{++} + G^{--} &= G^{+-} + G^{-+}, \\ G^{++}(t, t') - G^{--}(t, t') &= \text{sign}(t - t') [G^{-+}(t, t') - G^{+-}(t, t')]. \end{aligned} \quad (3.22)$$

### 3.3.2 Self correlation

We define the macroscopic two-time correlation as

$$C(t, t') \equiv \frac{1}{N} \sum_{i=1}^N \frac{1}{2} \langle \mathbf{n}_i^+(t) \cdot \mathbf{n}_i^-(t') + \mathbf{n}_i^-(t) \cdot \mathbf{n}_i^+(t') \rangle \quad (3.23)$$

$$= \frac{i\hbar}{2} [G^{+-}(t, t') + G^{-+}(t, t')] = \frac{i\hbar}{2} [G^{--}(t, t') + G^{++}(t, t')]. \quad (3.24)$$

It is symmetric in its time arguments  $C(t, t') = C(t', t)$ . Given the constraint  $\mathbf{n}(t) \cdot \mathbf{n}(t) = 1$ , it is one at equal times:  $C(t, t) = 1$ . The two-time correlation function is the simplest non-trivial quantity giving information on the dynamics of a system. In particular, a loss of its time translational invariance (TTI) is a signature of aging.

### 3.3.3 Self linear response

The response at time  $t$  of the observable  $n_i^\mu$  to an infinitesimal perturbation performed at a previous time  $t'$  on an observable  $f_i^\mu$  linearly coupled to  $n_i^\mu$  is defined as

$$R_i^\mu(t, t') \equiv \left. \frac{\delta \langle n_i^\mu(t) \rangle}{\delta f_i^\mu(t')} \right|_{f_i^\mu=0}, \quad (3.25)$$

with the modified Hamiltonian

$$H \mapsto H - f_i^\mu n_i^\mu. \quad (3.26)$$

Causality ensures that the response vanishes if  $t < t'$ . We define the macroscopic linear response as

$$R(t, t') = \frac{1}{N} \sum_{i=1}^N \sum_{\mu=1}^M R_i^\mu(t, t'). \quad (3.27)$$

The functional derivative with respect to  $f_i^\mu(t')$  in eq. (3.25) can be written in terms of the source fields  $\eta_i^{\mu\pm}(t')$  since  $f_i^\mu$  appears to play a similar role in the action functional:

$$\frac{\delta}{\delta f_i^\mu(t')} \longleftrightarrow \frac{1}{\hbar} \left( \frac{\delta}{\delta \eta_i^{\mu+}(t')} - \frac{\delta}{\delta \eta_i^{\mu-}(t')} \right). \quad (3.28)$$

Therefore we obtain a Kubo relation, stating that the response can be expressed in terms of two-time Green's functions:

$$\begin{aligned} R(t, t') &= -\frac{1}{N} \sum_{i=1}^N \sum_{\mu=1}^M \frac{i}{\hbar} \frac{1}{\mathcal{Z}} \left( \left. \frac{\delta^2 \mathcal{Z}[\boldsymbol{\eta}^\pm]}{\delta \eta_i^{\mu a}(t) \delta \eta_i^{\mu+}(t')} \right|_{\boldsymbol{\eta}^\pm=\mathbf{0}} - \left. \frac{\delta^2 \mathcal{Z}[\boldsymbol{\eta}^\pm]}{\delta \eta_i^{\mu a}(t) \delta \eta_i^{\mu-}(t')} \right|_{\boldsymbol{\eta}^\pm=\mathbf{0}} \right) \\ &= G^{a-}(t, t') - G^{a+}(t, t') \text{ with } a = + \text{ or } - \text{ equivalently} \\ &= \frac{1}{2} [G^{--}(t, t') + G^{+-}(t, t') - G^{++}(t, t') - G^{-+}(t, t')] \\ &= [G^{+-}(t, t') - G^{-+}(t, t')] \Theta(t - t'), \end{aligned} \quad (3.29)$$

where we made use of the relations (3.21).

Finally the four Keldysh Green's functions  $G^{ab}(t, t')$  can be re-expressed in terms of a couple of physical observables (namely correlation and response):

$$i\hbar G^{ab}(t, t') = C(t, t') - \frac{i\hbar}{2} [aR(t', t) + bR(t, t')]. \quad (3.30)$$

### 3.3.4 Keldysh rotation

The Keldysh rotation of the fields is a change of basis that simplifies the expressions of the physical observables such as the correlation  $C$  and the response  $R$  in terms of Green's functions. Moreover the connection with the Martin-Siggia-Rose generating functional in the classical limit is more straightforward in this representation [26, 31]. One introduces new fields as

$$\begin{cases} 2 \mathbf{n}_i^{(1)} &\equiv \mathbf{n}_i^+ + \mathbf{n}_i^-, \\ \hbar \mathbf{n}_i^{(2)} &\equiv \mathbf{n}_i^+ - \mathbf{n}_i^-, \end{cases} \quad (3.31)$$

and the inversion relation

$$\mathbf{n}_i^a = \mathbf{n}_i^{(1)} + a \frac{\hbar}{2} \mathbf{n}_i^{(2)}. \quad (3.32)$$

We define the Green's functions of these new fields as  $i\hbar G^{rs}(t, t') \equiv 1/N \sum_{i=1}^N \langle \mathbf{n}_i^r(t) \cdot \mathbf{n}_i^s(t') \rangle$  with  $r, s = (1), (2)$ . We have

$$\begin{aligned} i\hbar G^{(11)}(t, t') &= C(t, t'), & i\hbar G^{(12)}(t, t') &= -iR(t, t'), \\ i\hbar G^{(21)}(t, t') &= -iR(t', t), & i\hbar G^{(22)}(t, t') &= 0. \end{aligned} \quad (3.33)$$

The fact that  $G^{(22)}$  vanishes identically is very general and can be tracked back to be a consequence of causality. The unit length constraint imposed on the rotor coordinates,  $\mathbf{n}_i^a(t) \cdot \mathbf{n}_i^a(t) = 1$ , becomes an orthogonality constraint between the fields in the new basis,  $\mathbf{n}_i^{(1)}(t) \cdot \mathbf{n}_i^{(2)}(t) = 0$ , and a relation between their norms:  $\mathbf{n}_i^{(1)}(t)^2 + \frac{\hbar^2}{4} \mathbf{n}_i^{(2)}(t)^2 = 1$ .

### 3.3.5 Bosonic FDT

When the system of rotors is in equilibrium at a given temperature  $\beta^{-1}$ , the fluctuation-dissipation theorem (FDT) holds (in its bosonic version) giving an extra relation between the Green's functions. In Fourier space (see Appendix A for our Fourier conventions) it reads

$$C(\omega) = \hbar \coth(\beta\hbar\omega/2) \text{Im} R(\omega). \quad (3.34)$$

For completeness, we derive this theorem in Appendix D.2.

## 4 The influence of the fermion baths

### 4.1 Self-energy

We treat the interactions with the environment in perturbation theory up to second order in the coupling. After the fermionic degrees of freedom are integrated out, the resulting effective action for the rotors acquires an extra term encoding the effects of the reservoirs. The detailed computation, given in Appendix D.1, yields

$$S_{\text{eff}} = S_S + S_{\text{LM}} + S_{SB}^{(2)}, \quad (4.1)$$

with

$$\frac{i}{\hbar} S_{SB}^{(2)}[\mathbf{s}^{(1)}, \mathbf{s}^{(2)}] = \frac{1}{2} M \sum_{rs=(1),(2)} \iint_0^\infty dt dt' \Sigma_B^{rs}(t, t') \sum_{i=1}^N \mathbf{n}_i^r(t) \cdot \mathbf{n}_i^s(t'), \quad (4.2)$$

and the four self-energy components

$$\Sigma_B^{(22)} = 2(\hbar\omega_c)^2 \text{Re} [G_L^K G_R^{K*} - \hbar^2/4 (G_L^A G_R^{A*} + G_L^R G_R^{R*})] \equiv -\Sigma_B^K, \quad (4.3)$$

$$\Sigma_B^{(21)} = -2i(\hbar\omega_c)^2 \text{Re} [G_L^R G_R^{K*} + G_L^K G_R^{R*}] \equiv i\Sigma_B^R, \quad (4.4)$$

$$\Sigma_B^{(12)} = 2i(\hbar\omega_c)^2 \text{Re} [G_L^A G_R^{K*} + G_L^K G_R^{A*}] \equiv -i\Sigma_B^A, \quad (4.5)$$

$$\Sigma_B^{(11)} = 0. \quad (4.6)$$

The fact that  $\Sigma_B^{(11)}$  vanishes identically is a consequence of causality. Similarly to what we have done in Sect. 3.3.4 we renamed  $\Sigma_B^{(22)}$ ,  $\Sigma_B^{(21)}$  and  $\Sigma_B^{(12)}$  into  $\Sigma_B^K$ ,  $\Sigma_B^R$  and  $\Sigma_B^A$ . These real functions are usually referred to as the Keldysh, retarded and advanced components of the self-energy.  $G_\alpha^K$ ,  $G_\alpha^R$  and  $G_\alpha^A$  are the Keldysh, retarded and advanced Green's functions of the free electrons in the  $\alpha$ -reservoir respectively (see Appendix B.1). Using their properties under time reversal (see Appendix B.2), we establish

$$\Sigma_B^K(\tau) = \Sigma_B^K(-\tau), \quad \Sigma_B^R(\tau) = -\Sigma_B^A(-\tau). \quad (4.7)$$

These relations reduce the number of independent self-energy components to two (namely  $\Sigma_B^K$  and  $\Sigma_B^R$ ). Plugging the expressions of the fermionic Green's functions given in Appendix B.1, we obtain

$$\Sigma_B^K(\tau) = -\frac{1}{2}(\hbar\omega_c)^2 \langle\langle \left[ \tanh\left(\beta\frac{\epsilon_L - \mu_L}{2}\right) \tanh\left(\beta\frac{\epsilon_R - \mu_R}{2}\right) - 1 \right] \cos\left(\frac{\epsilon_L - \epsilon_R}{\hbar}\tau\right) \rangle_L \rangle_R, \quad (4.8)$$

$$\Sigma_B^R(\tau) = \frac{1}{\hbar}(\hbar\omega_c)^2 \langle\langle \left[ \tanh\left(\beta\frac{\epsilon_L - \mu_L}{2}\right) - \tanh\left(\beta\frac{\epsilon_R - \mu_R}{2}\right) \right] \sin\left(\frac{\epsilon_L - \epsilon_R}{\hbar}\tau\right) \rangle_L \rangle_R \Theta(\tau). \quad (4.9)$$

The notation  $\langle\langle \cdots \rangle_L \rangle_R$  stands for  $\int d\epsilon_L d\epsilon_R \rho_L(\epsilon_L) \rho_R(\epsilon_R) \cdots$ . The Fourier transforms read

$$\Sigma_B^K(\omega) = -\frac{1}{2}\pi\hbar(\hbar\omega_c)^2 \langle\langle \left[ \tanh\left(\beta\frac{\epsilon_L - \mu_L}{2}\right) \tanh\left(\beta\frac{\epsilon_R - \mu_R}{2}\right) - 1 \right] \times [\delta(\hbar\omega - \epsilon_{LR}) + \delta(\hbar\omega + \epsilon_{LR})] \rangle_L \rangle_R, \quad (4.10)$$

$$\text{Re } \Sigma_B^R(\omega) = -(\hbar\omega_c)^2 \langle\langle \left[ \tanh\left(\beta\frac{\epsilon_L - \mu_L}{2}\right) - \tanh\left(\beta\frac{\epsilon_R - \mu_R}{2}\right) \right] \text{pv} \frac{\epsilon_{LR}}{(\hbar\omega)^2 - \epsilon_{LR}^2} \rangle_L \rangle_R,$$

$$\text{Im } \Sigma_B^R(\omega) = \frac{1}{2}\pi\hbar(\hbar\omega_c)^2 \langle\langle \left[ \tanh\left(\beta\frac{\epsilon_L - \mu_L}{2}\right) - \tanh\left(\beta\frac{\epsilon_R - \mu_R}{2}\right) \right] \times [\delta(\hbar\omega - \epsilon_{LR}) - \delta(\hbar\omega + \epsilon_{LR})] \rangle_L \rangle_R, \quad (4.11)$$

where  $\epsilon_{LR} \equiv \epsilon_L - \epsilon_R$ . Since  $\Sigma_B^K(\tau)$  is a real and even function of  $\tau$ ,  $\Sigma_B^K(\omega)$  is also a real and even function of  $\omega$ .  $\Sigma_B^R(\tau)$  being real,  $\Sigma_B^R(\omega)$  is Hermitian:  $\Sigma_B^R(\omega) = \Sigma_B^R(-\omega)^*$ .

## 4.2 Some limits

Expressions (4.10) and (4.11) of the Keldysh and retarded self-energies are somehow cumbersome. We simplify them here in some physical limits. These expressions are heavily used in the rest of this work.

### 4.2.1 Zero drive

The  $L$  and  $R$  reservoirs constitute an equilibrium bath for the rotors as soon as they share the same temperature and the strength of the drive is set to zero ( $\mu_L = \mu_R$ ,  $eV = 0$ ). In this case, the fluctuation-dissipation theorem applies to the bath, and gives an extra relation between the bath self-energy components. It reads

$$\Sigma_B^K(\omega) = \hbar \coth\left(\beta\frac{\hbar\omega}{2}\right) \text{Im } \Sigma_B^R(\omega). \quad (4.12)$$

Ultimately the number of independent self-energy components reduces to one. We checked in Appendix D.2 that the expressions (4.10) and (4.11) comply with the FDT in the equilibrium case.

### 4.2.2 Low frequency

Let us consider the low frequency limit ( $\omega \rightarrow 0$ ), or long time-difference in real time, of the self-energy components of a generic non-equilibrium bath ( $eV \neq 0$  *a priori*). Parity considerations on  $\Sigma_B^K$  and  $\Sigma_B^R$  show that  $\Sigma_B^K(\omega)$  approaches  $\Sigma_B^K(\omega = 0)$  which depends on  $T$ ,  $eV$  and  $\epsilon_F$  whereas  $\text{Im} \Sigma_B^R(\omega) \propto \omega$ . The low frequency limit, which can also be seen as the classical limit ( $\hbar\omega \ll T$ ) of the quantum fluctuation-dissipation theorem in eq. (4.12) gives a way to express the temperature of an equilibrium bath as

$$T = \lim_{\omega \rightarrow 0} \frac{1}{2} \frac{\Sigma_B^K(\omega)}{\partial_\omega \text{Im} \Sigma_B^R(\omega)}. \quad (4.13)$$

By analogy with the equilibrium case, we introduce for non-equilibrium situations

$$T^* \equiv \lim_{\omega \rightarrow 0} \frac{1}{2} \frac{\Sigma_B^K(\omega)}{\partial_\omega \text{Im} \Sigma_B^R(\omega)}. \quad (4.14)$$

We expect that the effect of the reservoirs on the long time-difference dynamics of the rotors is the one of an equilibrium bath at temperature  $T^*$ .

### 4.2.3 $\epsilon_F$ much larger than all other energy scales

The reservoirs act as an *Ohmic* bath in the limit in which  $\epsilon_F$  is much larger than the temperature, the drive and  $\hbar\omega$  ( $eV, T, \hbar\omega \ll \epsilon_F$ ). Equation (4.11) with  $\Delta\epsilon \equiv \epsilon_L - \epsilon_R$  reads

$$\begin{aligned} \text{Im} \Sigma_B^R(\omega) &= \frac{1}{2} \pi (\hbar\omega_c)^2 \int d\epsilon' \int d\Delta\epsilon \rho(\epsilon') \rho(\epsilon' - \Delta\epsilon) [\delta(\hbar\omega - \Delta\epsilon) - \delta(\hbar\omega + \Delta\epsilon)] \\ &\quad \times \left[ \tanh\left(\beta \frac{\epsilon' - \mu_0}{2}\right) - \tanh\left(\beta \frac{\hbar(\epsilon' - \Delta\epsilon) - \mu_0 - eV}{2}\right) \right]. \end{aligned} \quad (4.15)$$

In the limit  $\hbar\omega \ll \epsilon_F$ , we use  $\rho(\epsilon' \pm \hbar\omega) \simeq \rho(\epsilon')$  and we derive

$$\text{Im} \Sigma_B^R(\omega) \simeq \frac{1}{2} \pi (\hbar\omega_c)^2 \int d\epsilon' \rho^2(\epsilon') \left[ \tanh\left(\beta \frac{\epsilon' + \hbar\omega - \mu_0 - eV}{2}\right) - \tanh\left(\beta \frac{\epsilon' - \hbar\omega - \mu_0 - eV}{2}\right) \right].$$

The factor within the square brackets in the integrand is peaked at  $\epsilon' = \mu_0 + eV$ . Hence we can approximate  $\rho^2(\epsilon') \simeq \rho^2(\mu_0)$  and then compute the remaining integral exactly to obtain an Ohmic (in the sense that it is proportional to  $\omega$ ) behavior for the imaginary part of the retarded self-energy:

$$\text{Im} \Sigma_B^R(\omega) \simeq 2\pi \hbar (\hbar\omega_c)^2 \rho^2(\mu_0) \omega. \quad (4.16)$$

Interesting enough, this expression is independent of  $T$  and  $V$ . Similar calculations give

$$\Sigma_B^K(\omega) \simeq 2\pi \hbar (\hbar\omega_c)^2 \rho^2(\mu_0) \frac{eV \sinh(\beta eV) - \hbar\omega \sinh(\beta \hbar\omega)}{\cosh(\beta eV) - \cosh(\beta \hbar\omega)}. \quad (4.17)$$

In order to determine  $T^*$ , we investigate the low frequency limit of  $\Sigma_B^K(\omega)$  given in eq. (4.17).



**Zero drive.** For  $eV \ll T \ll \epsilon_F$ , eq. (4.17) yields

$$\Sigma_B^K(\omega) \simeq 2\pi\hbar^2(\hbar\omega_c)^2\rho^2(\mu_0) \omega \coth(\beta\hbar\omega/2). \quad (4.18)$$

Equations (4.16) and (4.18) are linked through FDT. In the low frequency limit ( $\hbar\omega, eV \ll T \ll \epsilon_F$ ) it reads

$$\Sigma_B^K(\omega) \simeq 4\pi\hbar(\hbar\omega_c)^2\rho^2(\mu_0) T, \quad (4.19)$$

yielding  $T^* = T$  as expected in this equilibrium situation.

**Finite drive.** As soon as the drive is not negligible compared to temperature, in the low frequency regime ( $\hbar\omega \ll T \ll \epsilon_F$  and  $eV \ll \epsilon_F$ )

$$\Sigma_B^K(\omega) \simeq 2\pi\hbar(\hbar\omega_c)^2\rho^2(\mu_0) eV \coth(\beta eV/2), \quad (4.20)$$

yielding

$$T^* = \frac{eV}{2} \coth(\beta eV/2). \quad (4.21)$$

An ‘‘FDT like’’ relation is verified in these limits

$$\Sigma_B^K(\omega) = \hbar \coth(\hbar\omega/2T^*) \text{Im} \Sigma_B^R(\omega). \quad (4.22)$$

A similar interpretation of the effect of a two-leads bath in these limits on the dynamics of a single localized spin was given in [33] and [34].

Furthermore, in the low temperature limit ( $\hbar\omega \ll T \ll eV \ll \epsilon_F$ )

$$\Sigma_B^K(\omega) \simeq 2\pi\hbar(\hbar\omega_c)^2\rho^2(\mu_0) |eV|, \quad (4.23)$$

yielding  $T^* \equiv |eV|/2$ .

Finally in the zero temperature limit ( $0 = T \ll \hbar\omega, eV \ll \epsilon_F$ )

$$\Sigma_B^K(\omega) = 2\pi\hbar(\hbar\omega_c)^2\rho^2(\mu_0) \begin{cases} |eV| & \text{if } |\hbar\omega| \leq |eV|, \\ |\hbar\omega| & \text{if } |\hbar\omega| > |eV|. \end{cases} \quad (4.24)$$

In the low frequency regime, we recover expression (4.23). In the zero temperature and zero drive limit ( $0 = T = eV \ll \hbar\omega \ll \epsilon_F$ ) the Keldysh component of the bath self-energy reads  $\Sigma_B^K(\omega) = 2\pi\hbar(\hbar\omega_c)^2\rho^2(\mu_0) |\hbar\omega|$  that goes linearly to zero in the  $\hbar\omega \rightarrow 0$  limit.

#### 4.2.4 Zero temperature

In the  $T = 0$  limit, we obtain for finite values of the other parameters ( $eV, \hbar\omega, \epsilon_F$ )

$$\Sigma_B^K(\omega) = \pi\hbar(\hbar\omega_c)^2 \left[ \text{sign}(eV + \hbar\omega) \int_{\mu_0}^{\mu_0+eV+\hbar\omega} d\epsilon \rho(\epsilon)\rho(\epsilon - \hbar\omega) + \text{sign}(eV - \hbar\omega) \int_{\mu_0}^{\mu_0+eV-\hbar\omega} d\epsilon \rho(\epsilon)\rho(\epsilon + \hbar\omega) \right], \quad (4.25)$$

$$\text{Im} \Sigma_B^R(\omega) = \pi(\hbar\omega_c)^2 \left[ \int_{\mu_0}^{\mu_0+eV+\hbar\omega} d\epsilon \rho(\epsilon)\rho(\epsilon - \hbar\omega) - \int_{\mu_0}^{\mu_0+eV-\hbar\omega} d\epsilon \rho(\epsilon)\rho(\epsilon + \hbar\omega) \right]. \quad (4.26)$$

In the low frequency limit ( $0 = T \ll \hbar\omega \ll eV, \epsilon_F$ ) they yield

$$\Sigma_B^K(\omega) \simeq 2\pi\hbar(\hbar\omega_c)^2 \text{sign}(eV) \int_{\mu_0}^{\mu_0+eV} d\epsilon \rho^2(\epsilon), \quad (4.27)$$

$$\text{Im} \Sigma_B^R(\omega) \simeq \pi\hbar(\hbar\omega_c)^2 [\rho^2(\mu_0) + \rho^2(\mu_0 + eV)] \omega, \quad (4.28)$$

so that

$$T^*(T=0) = \text{sign}(eV) \frac{\int_{\mu_0}^{\mu_0+eV} d\epsilon \rho^2(\epsilon)}{\rho^2(\mu_0) + \rho^2(\mu_0 + eV)}. \quad (4.29)$$

#### 4.2.5 Some specific reservoirs

For the half-filled semi-circular DOS (type A), at zero drive and zero temperature, we establish the following analytical results at finite  $\epsilon_F$ :

$$\Sigma_B^K(\tau) = 2 \left( \frac{\hbar\omega_c}{\epsilon_F} \right)^2 \frac{J_1^2(\tau\epsilon_F/\hbar) - S_1^2(\tau\epsilon_F/\hbar)}{(\tau/\hbar)^2}, \quad (4.30)$$

$$\Sigma_B^R(\tau) = \frac{8}{\hbar} \left( \frac{\hbar\omega_c}{\epsilon_F} \right)^2 \frac{J_1(\tau\epsilon_F/\hbar)S_1(\tau\epsilon_F/\hbar)}{(\tau/\hbar)^2} \Theta(\tau), \quad (4.31)$$

with  $\Sigma_B^R(\tau=0) = 0$ ,  $\Sigma_B^K(\tau=0) = \frac{1}{2}(\hbar\omega_c)^2$ .  $J_1$  and  $S_1$  are the Bessel and the Struve functions of first kind and first order, respectively. From eqs. (4.30) and (4.31), we see that the temporal extent of both  $\Sigma_B^R$  and  $\Sigma_B^K$  is of order  $\hbar/\epsilon_F$ . In the limit in which  $\epsilon_F$  is much larger than any other energy scale, a numerical analysis shows that this property holds for finite values of the temperature and the drive as well. As a way of summary, in Fig. 6 (a) we plot  $\Sigma_B^K$  as a function of  $\tau\epsilon_F$  for  $\epsilon_F = 10J, 100J$  and at  $(T=J, V=0)$  and  $(T=0, V=J)$ . In the case in which  $\epsilon_F$  is finite, one can compute  $T^*$  for the half-filled semi-circular DOS at zero temperature:

$$T^*(T=0) = \frac{|eV|}{2} \frac{1 - 1/3 (eV/\epsilon_F)^2}{1 - 1/2 (eV/\epsilon_F)^2} \text{ for } |eV| < eV_{max} = \epsilon_F. \quad (4.32)$$

In Fig. 6 (b) we give a numerical integration of  $\text{Im} \Sigma_B^R(\omega)$  for the three types of reservoirs we introduced in Sect. 2.2 and in the case in which  $\epsilon_F$  is the largest energy scale. This shows that the self-energy is indeed the one of an Ohmic bath. The fact that their Ohmic behavior is approximately valid until  $\hbar\omega = \epsilon_F$  supports the property that the temporal extent of the self-energies (in real time) is of the order of  $\hbar/\epsilon_F$ .

## 5 Results

In this section we present our results. We first complete the calculation of disorder averaged generating function and, from it, we derive Schwinger-Dyson equations for the two-time correlation and linear response valid for all values of the parameters. We next derive the dynamical phase diagram as a function of the temperature of the reservoirs ( $T$ ), the strength of quantum

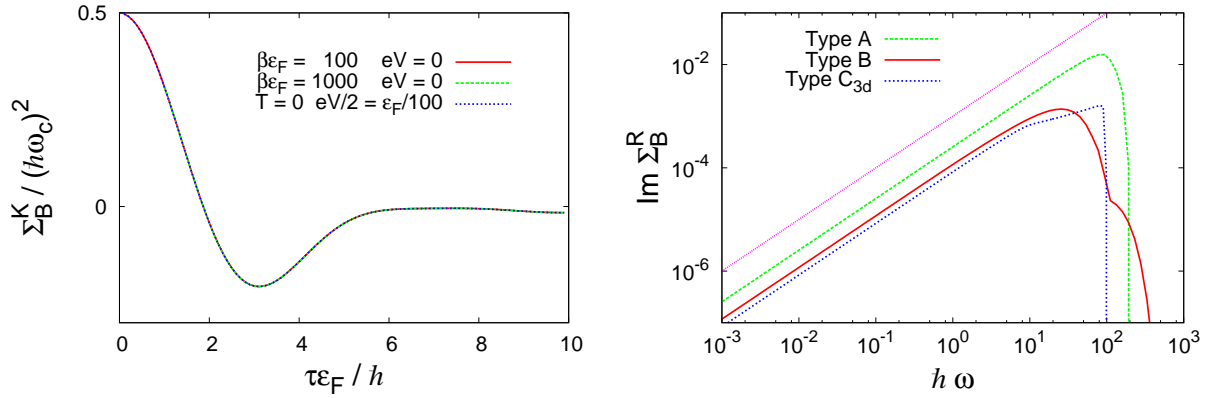


Figure 6: (Color online.) (a)  $\Sigma_B^K$  (for the half-filled semi-circle DOS) as a function of  $\tau\epsilon_F$  in the regime where  $\epsilon_F$  is much larger than any other energy scale: for  $\beta\epsilon_F = 100$  and  $\beta\epsilon_F = 1000$  at  $eV = 0$  and also for  $eV/2 = \epsilon_F/100$  at  $T = 0$ . The three curves are indistinguishable. This shows that  $\Sigma_B^K$  is indeed a function of  $\tau\epsilon_F$  in this regime and shows furthermore that  $eV/2$  plays the same role as  $T$ . (b)  $\text{Im } \Sigma_B^R(\omega)$  is represented in a double logarithmic scale for the three following DOSs with  $\beta\epsilon_F = \epsilon_F/eV = 100$ : the half-filled semi-circle  $\rho_A(\epsilon)$ , the half-filled type B with  $\rho_B(\epsilon)$  and the 3d free electrons DOS  $\rho_{C3d}(\epsilon)$ . The straight line above all is a guide to the eyes for a pure Ohmic ( $\propto \omega$ ) behavior. The rapid decay above  $\hbar\omega \sim \epsilon_F$  is a signature of the energy cut-off,  $\epsilon_{cut} \propto \epsilon_F$ , of the DOS.

fluctuations ( $\Gamma$ ), the voltage ( $eV$ ) and the coupling to the leads for which we introduce the new dimensionless parameter  $g \equiv \hbar\omega_c/\epsilon_F$ . We distinguish two phases separated by a second order phase transition. For high values of the temperature and/or strong drive and/or strong quantum fluctuations, we find a non-equilibrium steady state that approaches the usual paramagnet when  $eV \rightarrow 0$ . Whereas for low temperatures and/or low drive and/or quantum fluctuations we find a coarsening phase.

## 5.1 Average over disorder

At this stage, after tracing out all fermionic degrees of freedom, the effective action of our system is quadratic in the fields and reads

$$\begin{aligned}
\frac{i}{\hbar} S_{\text{eff}} = M \sum_{i=1}^N \int dt \left\{ \frac{i}{\Gamma} \dot{\mathbf{n}}_i^{(1)}(t) \cdot \dot{\mathbf{n}}_i^{(2)}(t) + \frac{i}{\sqrt{N}} \sum_{j<i}^N J_{ij} \left[ \mathbf{n}_i^{(1)}(t) \cdot \mathbf{n}_j^{(2)}(t) + \mathbf{n}_i^{(2)}(t) \cdot \mathbf{n}_j^{(1)}(t) \right] \right. \\
- \frac{1}{2} \int dt' \Sigma_B^K(t-t') \mathbf{n}_i^{(2)}(t) \cdot \mathbf{n}_i^{(2)}(t') + i \int dt' \Sigma_B^R(t-t') \mathbf{n}_i^{(2)}(t) \cdot \mathbf{n}_i^{(1)}(t') \\
\left. + \frac{i}{2\hbar} \sum_{a=\pm} a z_i^a(t) \left[ 1 - \frac{1}{2} \left( \mathbf{n}_i^{(1)}(t) \right)^2 - a\hbar \mathbf{n}_i^{(1)}(t) \cdot \mathbf{n}_i^{(2)}(t) - \frac{\hbar^2}{4} \left( \mathbf{n}_i^{(2)}(t) \right)^2 \right] \right\}. \quad (5.1)
\end{aligned}$$

Given that the initial condition for the rotors is taken to be uncorrelated with the disorder configuration (the  $J_{ij}$ 's), neither the initial density matrix  $\varrho(0)$  nor the generating functional without sources ( $\mathcal{Z}[\boldsymbol{\eta}^\pm = 0] = 1$ ) depend upon disorder. This property allows us to write dynamic equations by averaging over disorder the generating functional itself hence without

resorting to the use of replicas [31]. As in other quantum systems with quenched disorder [29, 31, 35, 37], we are therefore interested in

$$\overline{\mathcal{Z}[\boldsymbol{\eta}^\pm]}^J \equiv \int \left( \prod_{i,j < i} dJ_{ij} P(J_{ij}) \right) \mathcal{Z}[\boldsymbol{\eta}^\pm], \quad (5.2)$$

where  $P(J_{ij})$  is the Gaussian density distribution for the rotor couplings with zero mean and variance  $J^2$ . The disorder average over a random Gaussian potential can be readily done and the effective action of the system is quartic in the fields and reads

$$\begin{aligned} \frac{i}{\hbar} S_{\text{eff}} = M \sum_{i=1}^N \int dt \left\{ \frac{i}{\Gamma} \dot{\mathbf{n}}_i^{(1)}(t) \cdot \dot{\mathbf{n}}_i^{(2)}(t) \right. & (5.3) \\ & - \frac{J^2 M}{2N} \int dt' \sum_j \left[ \mathbf{n}_i^{(1)}(t) \cdot \mathbf{n}_j^{(2)}(t) \right] \left[ \mathbf{n}_i^{(1)}(t') \cdot \mathbf{n}_j^{(2)}(t') + \mathbf{n}_i^{(2)}(t') \cdot \mathbf{n}_j^{(1)}(t') \right] \\ & - \frac{1}{2} \int dt' \Sigma_B^K(t-t') \mathbf{n}_i^{(2)}(t) \cdot \mathbf{n}_i^{(2)}(t') + i \int dt' \Sigma_B^R(t-t') \mathbf{n}_i^{(2)}(t) \cdot \mathbf{n}_i^{(1)}(t') \\ & \left. + \frac{i}{2\hbar} \sum_{a=\pm} a z_i^a(t) \left[ 1 - \frac{1}{2} \left( \mathbf{n}_i^{(1)}(t) \right)^2 - a\hbar \mathbf{n}_i^{(1)}(t) \cdot \mathbf{n}_i^{(2)}(t) - \frac{\hbar^2}{4} \left( \mathbf{n}_i^{(2)}(t) \right)^2 \right] \right\}. \end{aligned}$$

## 5.2 Schwinger-Dyson equations

In the large  $M$  limit, we show that the Lagrange multipliers are homogeneous,

$$z_i^+(t) = z_i^-(t) \equiv z(t) \quad \forall i, t. \quad (5.4)$$

See Appendix E for a detailed computation. Moreover, introducing

$$\Sigma^K \equiv J^2 C + \Sigma_B^K, \quad \Sigma^R \equiv J^2 R + \Sigma_B^R, \quad (5.5)$$

we obtain the Schwinger-Dyson equations which fully determine the dynamics of the system:

$$\left[ \frac{1}{\Gamma} \frac{\partial^2}{\partial t^2} + z(t) \right] C(t, t') = \int_0^{t'} dt'' \Sigma^K(t, t'') R(t', t'') + \int_0^t dt'' \Sigma^R(t, t'') C(t'', t'), \quad (5.6)$$

$$\left[ \frac{1}{\Gamma} \frac{\partial^2}{\partial t^2} + z(t) \right] R(t, t') = \delta(t - t') + \int_{t'}^t dt'' \Sigma^R(t, t'') R(t'', t'), \quad (5.7)$$

$$z(t) = \int_0^t dt'' \Sigma^K(t, t'') R(t, t'') + \Sigma^R(t, t'') C(t, t'') - \frac{1}{\Gamma} \frac{\partial^2 C}{\partial t^2}(t, t' \rightarrow t^-). \quad (5.8)$$

We remark that the expression for the response is decoupled from the self correlation apart from a residual coupling through the Lagrange multiplier. This is actually a consequence of two features of the model: the disordered potential is quadratic in the rotors and the coupling to the reservoirs is linear in the rotors. The ‘‘initial’’ conditions are given by

$$C(t, t) = 1, \quad R(t, t) = 0 \quad \forall t. \quad (5.9)$$

Moreover, integrating eqs. (5.6) and (5.7) over an infinitesimal interval around  $t' = t$ , one sees that the first derivative of the correlation is continuous at equal times

$$\lim_{t' \rightarrow t^-} \partial_t C(t, t') = \lim_{t' \rightarrow t^+} \partial_t C(t, t') = 0, \quad (5.10)$$

whereas the one of the response function is discontinuous

$$\lim_{t' \rightarrow t^-} \partial_t R(t, t') = \Gamma, \quad \lim_{t' \rightarrow t^+} \partial_t R(t, t') = 0. \quad (5.11)$$

The structure of these equations is the same as the one in other out of equilibrium problems studied in [29, 31, 35, 37, 40].

### 5.3 Quantum non-equilibrium steady state (QNESS) phase

One expects that if the system is quenched into the high temperature phase, after a short transient it should relax toward a quantum non-equilibrium steady state (QNESS). The system of rotors cannot be in equilibrium since, for  $V \neq 0$ , an electronic current is passing through it. Nevertheless the dynamics are still stationary (time translationally invariant). This implies that  $C(t, t')$  and  $R(t, t')$  are only functions of  $t - t'$ . Guided by a numerical analysis (see Sect. 5.5.5), we make the assumption (that we later check to be consistent) that the quantity  $z(t)$  is a one-time observable that converges toward a finite value  $z^\infty$ . In this situation, one can Fourier transform the Schwinger-Dyson equations (5.6) and (5.7) with respect to  $t - t'$  to find

$$R(\omega) = \frac{1}{-\Gamma^{-1}\omega^2 + z^\infty - \Sigma^R(\omega)}, \quad (5.12)$$

$$C(\omega) = \Sigma^K(\omega) |R(\omega)|^2, \quad (5.13)$$

$$C(\omega) = \frac{\Sigma_B^K(\omega)}{\text{Im } \Sigma_B^R(\omega)} \text{Im } R(\omega), \quad (5.14)$$

Using the fact that  $\lim_{\omega \rightarrow \infty} R(\omega)$  has to vanish, eq. (5.12) implies

$$R(\omega) = \frac{1}{2J^2} \left( -\Gamma^{-1}\omega^2 + z^\infty - \Sigma_B^R(\omega) + \sqrt{(-\Gamma^{-1}\omega^2 + z^\infty - \Sigma_B^R(\omega))^2 - 4J^2} \right). \quad (5.15)$$

We note that in the cases in which the DOS of the reservoirs have an energy cut-off  $\epsilon_{cut}$ ,

$$C(\omega) = \text{Im } R(\omega) = \Sigma_B^K(\omega) = \text{Im } \Sigma_B^R(\omega) = 0 \text{ for } \hbar\omega > \epsilon_{cut}. \quad (5.16)$$

## 5.4 Critical manifold

### 5.4.1 Equation for criticality

Approaching the putative critical manifold from the disordered phase, see Fig. 1, where after a short transient the system should be time translationally invariant, we look for a singularity in the Fourier transformed Schwinger-Dyson equations that would be the signature of the loss of time translational invariance and ultimately of a phase transition toward an out of equilibrium

behavior. Anticipating a second order phase transition scenario where the onset of criticality is characterized by long-wavelength instabilities, we inspect these equations at  $\omega = 0$ .

The constraint that rotors have a unit length  $C(t, t) = 1$  implies

$$\int_0^\infty \frac{d\omega}{2\pi} C(\omega) = \frac{1}{2}, \quad (5.17)$$

and replacing  $C(\omega)$  with its expression in eq. (5.14):

$$\int_0^\infty \frac{d\omega}{2\pi} \frac{\Sigma_B^K(\omega)}{\text{Im} \Sigma_B^R(\omega)} \text{Im} R(\omega) = \frac{1}{2}. \quad (5.18)$$

Equation (5.15) at  $\omega = 0$  reads

$$R(\omega = 0) = \frac{1}{2J^2} \left( z^\infty - \Sigma_B^R(\omega = 0) + \sqrt{(z^\infty - \Sigma_B^R(\omega = 0))^2 - 4J^2} \right). \quad (5.19)$$

$R(\omega = 0) = \int_0^\infty d\tau R(\tau)$  has to be real since  $R(\tau)$  is real<sup>2</sup>. However, it is clear from eq. (5.19) that  $z^\infty = z_c^\infty \equiv 2J + \Sigma_B^R(\omega = 0)$  is a singular point (a minus sign would be incoherent with the approach in Sect. 5.5). This is the signature of the phase transition we were looking for. At criticality,

$$R(\omega = 0)|_{z^\infty = z_c^\infty} = 1/J. \quad (5.20)$$

Concomitantly, the value of  $C(\omega = 0)$  blows up. Inserting  $z_c^\infty$  in eq. (5.18), we obtain the equation for the critical manifold,

$$\int_0^\infty \frac{d\omega}{2\pi} \frac{\Sigma_B^K(\omega)}{\text{Im} \Sigma_B^R(\omega)} \text{Im} R(\omega)|_{z_c^\infty} = \frac{1}{2}. \quad (5.21)$$

The parameters are the strength of quantum fluctuations  $\Gamma$ , the temperature  $T$ , the voltage applied between the two reservoirs  $V$ . We recall that  $J$  is the typical interaction between two rotors. The energy variation scale of the reservoirs is characterized by  $\epsilon_F$  and  $\hbar\omega_c$  quantifies the coupling strength of the rotors to their environment through the dimensionless small parameter  $g \equiv \hbar\omega_c/\epsilon_F$ .

In the rest of this Section, we use eq. (5.21) to uncover the phase diagram of Fig. 1. The critical surface is parametrized in the  $T, \Gamma, V$  space by  $T_c, \Gamma_c, V_c$  ( $g$  is kept constant). We introduce the critical points  $\bar{T}_c \equiv T_c(\Gamma = V = 0)$ ,  $\bar{V}_c \equiv V_c(T = \Gamma = 0)$ ,  $\bar{\Gamma}_c \equiv \Gamma_c(T = V = 0)$ . Anticipating the coming results, we introduce the dimensionless reduced parameters  $\theta \equiv T/J$ , and  $v \equiv eV/2J$ ,  $\gamma \equiv (4\hbar/3\pi)^2 \Gamma/J$ . In the plane  $V = 0$ , where the reservoirs act like an equilibrium bath, we recover the results in [29]. In the classical limit  $V = \Gamma = 0$ , we recover the ones in [30].

In the limit in which  $\epsilon_F$  is much larger than any other energy scale, using eqs. (4.16) and (4.17), the equation for the critical surface reads

$$\int_0^\infty \frac{d\omega}{2\pi} \frac{1}{\omega} \frac{eV \sinh(\beta eV) - \hbar\omega \sinh(\beta \hbar\omega)}{\cosh(\beta eV) - \cosh(\beta \hbar\omega)} \text{Im} R(\omega)|_{z_c^\infty} = \frac{1}{2}. \quad (5.22)$$

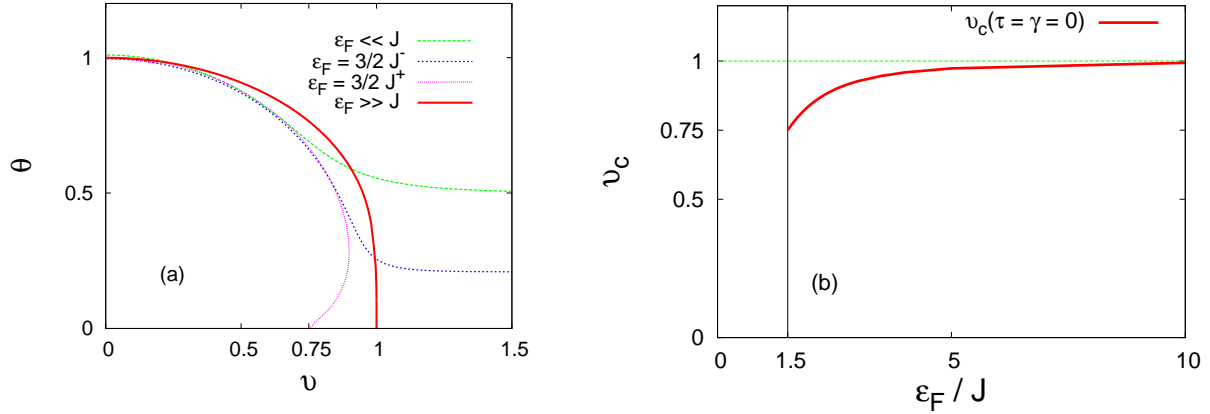


Figure 7: Study of the behavior of the  $\gamma = 0$  critical line with the ratio  $\epsilon_F/J$  for the half-filled semi-circle DOS. (a) The  $\gamma = 0$  critical line  $\theta_c(\nu)$  is given for four different values of the ratio  $\epsilon_F/J$ . The analytical expression of the  $\epsilon_F/J \rightarrow \infty$  curve is given in eq. (5.26). For  $\epsilon_F/J < 3/2$  the critical point  $\bar{\nu}_c$  is rejected to infinity. (b)  $\bar{\nu}_c \equiv \nu_c(\theta = \gamma = 0)$  is plotted against  $\epsilon_F/J$ . All these  $\gamma = 0$  results are independent of the value  $g$ .

#### 5.4.2 Critical points on the $\Gamma = 0$ plane

Taking the  $\Gamma \rightarrow 0$  limit of expression (5.15) one has

$$\text{Im } R(\omega')|_{z_c^\infty} = \begin{cases} \frac{1}{J} \sqrt{1 - (1 - \omega'^2)^2} & \text{for } \omega' \in [0, \sqrt{2}] , \\ 0 & \text{for } \omega' \geq \sqrt{2} , \end{cases} \quad (5.23)$$

where we introduced  $\omega' \equiv \omega/\sqrt{2J\Gamma}$ . The expression of  $\text{Im } R(\omega)$  does not involve the reservoirs: the time scale of the rotors (controlled by  $\Gamma$ ) totally decouples from the one of the reservoirs in such a way that the rotors only couple with the zero mode (the slowest) of the reservoirs. Using eq. (5.21), we write the equation of the critical manifold in the  $\Gamma = 0$  plane

$$\lim_{\Gamma \rightarrow 0} \sqrt{\frac{2\Gamma}{J}} \int_0^{\sqrt{2}} \frac{d\omega'}{2\pi} \sqrt{1 - (1 - \omega'^2)^2} \frac{\Sigma_B^K(\sqrt{2J\Gamma}\omega')}{\text{Im } \Sigma_B^R(\sqrt{2J\Gamma}\omega')} = \frac{1}{2} . \quad (5.24)$$

Using the definition (4.14) of  $T^*(T, eV)$  introduced in Sect. 4.2.2, this simply reads

$$T^*(T_c, eV_c) = J . \quad (5.25)$$

At  $eV = 0$ , for which the reservoirs constitute an equilibrium bath, the ratio  $\Sigma_B^K/\text{Im } \Sigma_B^R$  is given by the FDT and we find a temperature-induced classical critical point  $\bar{T}_c \equiv T_c(\Gamma = V = 0) = J$ . In terms of the reduced temperature this reads  $\bar{\theta}_c = 1$ . In the next two paragraphs we look at how this critical point is affected by a finite drive ( $eV \neq 0$ ).

**Infinite  $\epsilon_F$ .** We first consider the limit  $\epsilon_F \rightarrow \infty$ , using the explicit expression (4.21) for  $T^*$  one finds:

$$T_c(eV) = \frac{eV}{2} \Big/ \text{arccoth} \left( \frac{2J}{eV} \right) . \quad (5.26)$$

---

<sup>2</sup> $\Sigma_B^R(\omega = 0)$  is real for the same reason.

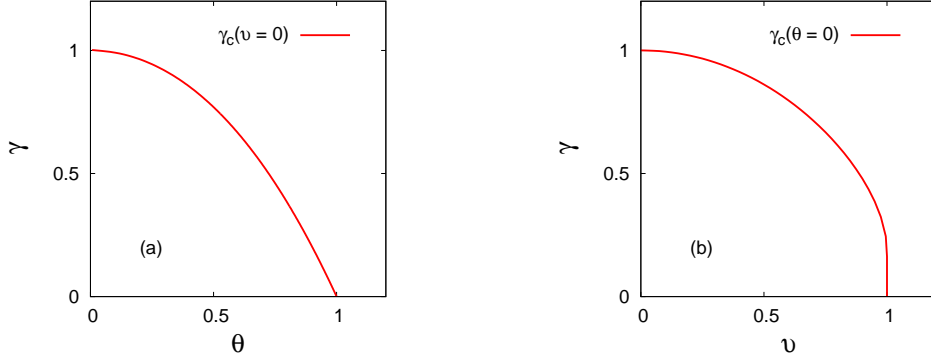


Figure 8: Phase diagram in terms of the reduced parameters analytically determined in the limit  $g \rightarrow 0$ . (a) Critical line for  $V = 0$ . (b) Critical line for  $T = 0$  in the limit  $\epsilon_F \rightarrow \infty$ .

From this equation we find a drive-induced critical point at  $e\bar{V}_c/2 = J$ . In terms of the reduced voltage this reads  $\bar{v}_c = 1$ . The departure from the classical critical temperature on the  $\gamma = 0$  plane is quadratic:  $\theta_c \simeq 1 - (1/3)v^2$  for  $v \ll 1$ . Instead, on the zero-drive plane,  $v = 0$ , the critical line leaves  $\bar{\theta}_c$  linearly:  $\theta_c \simeq 1 - (3\pi^2/16)\gamma$  for  $\gamma \ll 1$ . More details on the critical line  $\gamma_c(t)$  at  $v = 0$  are given in [27]. Close to  $\bar{v}_c$  on the  $\theta = 0$  and  $\gamma = 0$  planes the departure of the critical lines  $\gamma_c(v)$  and  $\theta_c(v)$ , respectively, are non-analytical and thus very steep [see Figs. 7 (a) and 8 (b)].

**Finite  $\epsilon_F$ .** Let us now investigate the  $T = 0$  critical point  $\bar{V}_c$  for finite values of  $\epsilon_F$ . For our simple DOS depending on a unique parameter  $\epsilon_F$ ,  $\bar{v}_c$  is controlled by  $\epsilon_F/J$ . Plugging the expression (4.29) for  $T^*(T = 0)$  into the expression (5.25) we obtain

$$\text{sign}(e\bar{V}_c) \frac{1}{J} \frac{\int_{\mu_0}^{\mu_0 + e\bar{V}_c} d\epsilon' \rho^2(\epsilon')}{\rho^2(\mu_0) + \rho^2(\mu_0 + e\bar{V}_c)} = 1. \quad (5.27)$$

The existence and the value of the solution  $\bar{V}_c$  depend on the details of the DOS  $\rho(\epsilon)$ . If the DOS has an energy cut-off  $\epsilon_{cut}$ , the existence of a solution is guaranteed if the cut-off is larger than the solution  $\epsilon_{cut}^{min}$  of

$$\int_{\mu_0}^{\epsilon_{cut}^{min}} d\epsilon \rho^2(\epsilon) = J\rho^2(\mu_0). \quad (5.28)$$

For the type A half-filled semi-circle distribution ( $\mu_0 = \epsilon_F$ ,  $\epsilon_{cut} = 2\epsilon_F$ ), it turns out that eq. (5.27) admits a finite solution as soon as  $\epsilon_F/J \geq 3/2$ . For  $\epsilon_F/J = 3/2$ , one finds  $e\bar{V}_c = 3/2 J$  ( $\bar{v}_c = 3/4$ ). For  $\epsilon_F/J > 3/2$ , the finite solution  $\bar{v}_c$  goes to one as one increases the ratio  $\epsilon_F/J$ . For  $\epsilon_F/J < 3/2$  the critical point is rejected to infinity and the critical line in the  $\Gamma = 0$  plane converges to the asymptotic value  $\theta_c(v \gg 1) = 1/2$  as  $\epsilon_F/J \rightarrow 0$ . See Fig. 7.

For the distribution B, if  $\mu_0 \neq 0$ , the scenario is the same as for the semi-circle distribution there is a finite value of the ratio  $\epsilon_F/J$  under which, the critical point  $\bar{v}_c$  is rejected to infinity, and above which,  $\bar{v}_c$  has a finite value that goes to 1 in the limit  $\epsilon_F \rightarrow \infty$ . If  $\mu_0 = 0$  then  $\bar{v}_c$  remains finite.



For the distribution of type C, eq. (5.27) always admits a finite solution  $\bar{v}_c$  independent of  $\epsilon_F$ . For the distribution C3d,  $\bar{v}_c = 1$  regardless of  $\mu_0$ ,  $\epsilon_F$  and  $J$ . For the distribution C2d, we also get  $\bar{v}_c = 1$ . For the distribution C1d, one can show that as long as  $\mu_0 > 0$ , there is a finite  $\bar{v}_c$ , function only of  $u \equiv J/\mu_0$ :  $\bar{v}_c = [\exp(u + L(ue^{-u})) - 1]/2u$ , where  $L(x)$  is the only solution of the equation  $Le^L = x$  that is analytic in 0. For  $\mu_0(\epsilon_F \rightarrow \infty) \rightarrow \infty$ , we recover  $\bar{v}_c = 1$ .

### 5.4.3 Quantum critical point

**Weak coupling limit.** We first consider the limit of the weak coupling to the reservoirs  $g \rightarrow 0$  after the long-time limit such that the asymptotic regime has been established. It is actually in this  $g \rightarrow 0$  limit that the self-energy was computed (we expanded the total action up to second order in  $g$ ) in Sect. 4.  $g \equiv \hbar\omega_c/\epsilon_F$  can be sent to zero by sending the coupling parameters to zero, but for our simple DOS, it can also be realized by sending  $\epsilon_F$  to infinity.

In equilibrium ( $V = 0$ ) at  $T = 0$ , the FDT gives

$$\frac{\Sigma_B^K(\omega)}{\text{Im} \Sigma_B^R(\omega)} = \hbar \text{ for } 0 < \hbar\omega < \epsilon_{cut} . \quad (5.29)$$

By turning off the coupling to the reservoirs ( $g \rightarrow 0$ ) in eq. (5.19) one has

$$\text{Im} R(\omega')|_{z_c^\infty} = \begin{cases} \frac{1}{J} \sqrt{1 - (1 - \omega'^2)^2} & \text{for } \omega' \in [0, \sqrt{2}] , \\ 0 & \text{for } \omega' \geq \sqrt{2} , \end{cases} \quad (5.30)$$

where we introduced  $\omega' \equiv \omega/\sqrt{2J\Gamma}$ . Plugging eqs. (5.29) and (5.30) in the equation for the critical manifold (5.21) gives the quantum critical point

$$\hbar^2 \bar{\Gamma}_c \equiv \left(\frac{3\pi}{4}\right)^2 J \text{ if } \epsilon_{cut} > \frac{3\pi}{2} J \text{ and no solution otherwise.} \quad (5.31)$$

For type A reservoirs in the  $\epsilon_F \rightarrow \infty$  limit, one can prove that the critical surface is parabolic close to the quantum critical point  $\bar{\gamma}_c$ , *i.e.*,  $\gamma_c \simeq 1 - (16/3\pi^2)\theta^2$  at  $\theta \ll 1$  and  $v = 0$ , and  $\gamma_c \simeq 1 - (16/3\pi^2)v^2$  for  $v \ll 1$  and  $\theta = 0$ .

**Finite coupling.** When the coupling to the electronic reservoirs  $g$  is finite this quantum critical point (actually the whole critical surface) moves upward when increasing the coupling constant (see Fig. 9). The coarsening phase is thus stabilized when increasing the coupling to the reservoirs. In the  $\epsilon_F \rightarrow \infty$  limit, one has for  $g \ll 1$

$$\bar{\gamma}_c \simeq 1 + 2 \left(\frac{3\pi}{4}\right)^2 (\hbar\omega_c)^2 \rho^2(\mu_0) . \quad (5.32)$$

In the case of the type A half-filled semi-circle distribution this reads  $\bar{\gamma}_c \simeq 1 + (9/2)g^2$ . This is similar to what was found for other quantum spin models embedded in an Ohmic harmonic oscillator bath and is due to a spin-localization-like effect [29, 35]. This similitude is not surprising since we showed in Sect. 4.2, eq. (4.16), that the mixed electronic reservoirs behave like an Ohmic bath in the  $\epsilon_F \rightarrow \infty$  limit.

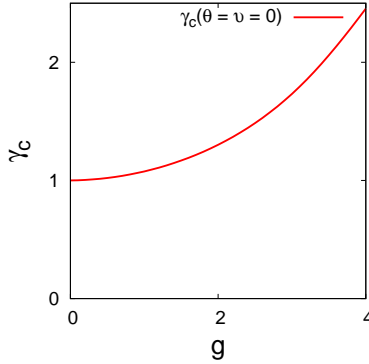


Figure 9: Numerical study of the evolution of the critical point  $\bar{\gamma}_c \equiv \gamma_c(\theta = 0, v = 0)$  with the coupling parameter  $g$  (here for  $\epsilon_F/J = 10$ ).

$\Gamma_c(V=0) \sim \bar{T}_c - T$	$T_c(\Gamma=0) \sim \text{NA}$	$V_c(T=0) \sim (\bar{\Gamma}_c - \Gamma)^{1/2}$
$\Gamma_c(T=0) \sim \text{NA}$	$T_c(V=0) \sim (\bar{T}_c - T)^{1/2}$	$V_c(\Gamma=0) \sim (\bar{T}_c - T)^{1/2}$

Table 1: Behavior of the critical manifold close to the critical points for  $g \rightarrow 0$  and  $\epsilon_F \rightarrow \infty$ . Close to the critical point  $\bar{V}_c = V_c(T = \Gamma = 0)$  the critical lines are non-analytical (NA).

#### 5.4.4 Summary of the phase diagram

Let us summarize the key features of the critical manifold in the case of a DOS with  $\epsilon_F \rightarrow \infty$ . When the coupling to the reservoir  $g$  is set to zero, the values of three critical points ( $\bar{T}_c, \bar{\Gamma}_c, e\bar{V}_c$ ) are only controlled by  $J$  that measures the disorder strength. Figure 1 gathers all the  $g \rightarrow 0$  results in the  $T, \Gamma, V$  space. The increase in either the thermal or quantum fluctuations, by raising  $\Gamma$  or the temperature  $T$ , respectively, leads to the destabilization of the coarsening phase. The same occurs for an increase in the bias voltage  $V$ . The summary of the behavior of the critical manifold close to the critical points  $\bar{T}_c, \bar{\Gamma}_c$  and  $\bar{V}_c$  is given in Table 1. Furthermore, an increase in the rotors-reservoirs coupling  $g$  pulls the quantum critical point  $\bar{\Gamma}_c$  upward (as indicated in Fig. 1 by a vertical arrow) enlarging the low temperature phase.

### 5.5 Coarsening phase

We study the dynamics in the low  $T$ , weak  $\Gamma$ , weak  $V$  region of the phase diagram by solving the Schwinger-Keldysh equations in two ways: with an exact numerical approach and using analytic approximation in the long-time dynamics. We prove that in this region of the phase diagram there is coarsening and that the aging dynamics that occur are universal and equivalent to the ones of the classical (and undriven) limit of our model (*a.k.a.* the  $p = 2$  spherical model with quenched disorder).

#### 5.5.1 Numerical solution

Our numerical analysis consists in solving the Schwinger-Dyson equations (5.6), (5.7) and (5.8) after a quench into the low temperature, weak quantumness, weak drive phase. Thanks to their

causal structure, the equations on  $C$ ,  $R$  and  $z$  can be integrated step by step in time, with a Runge-Kutta method. Apart from arbitrarily small numerical errors, this approach is exact.

We concentrate on reservoirs at temperature  $T$  that have a type A semi-circle DOS (both  $L$  and  $R$  reservoirs).  $L$  reservoirs are kept half-filled while a voltage  $V$  is applied between  $L$  and  $R$  reservoirs.  $\epsilon_F$  is chosen to be the largest energy scale. Typically, we consider the following values for the parameters:  $T \sim \Gamma \sim eV \sim 0.1J$  and  $\epsilon_F \sim 10J$ .

The analysis shows (analytical arguments are given in Sect. 5.5.3) that the dynamics after the quench below the critical surface do not reach a QNESS. There is a separation of two-time scales typical of aging phenomena [16]. The data in Figs. 10-12 were obtained using the algorithm briefly described.

### 5.5.2 Mapping to Langevin dynamics

The goal of this subsection is to map our quantum field theory description of the rotors dynamics, which involves the two fields  $\mathbf{n}^{(1)}$  and  $\mathbf{n}^{(2)}$  (see Sect. 3.3.4), to an equivalent description in terms of Langevin dynamics. In the long-time limit of the coarsening dynamics, we establish that the equation of motion for the field  $\mathbf{n}^{(1)}$  is actually a Langevin equation driven by a colored noise  $\boldsymbol{\xi}$  the statistical characteristics of which are controlled by the self-energies of the fermion reservoirs.

Let us take a step back and rewrite the effective action as it was before averaging over disorder. Making the assumption (we later check its consistency) that the Lagrange multipliers satisfy  $z_i^+(t) = z_i^-(t) = z_i(t) \forall i, t$ , the effective action reads

$$\begin{aligned} \frac{i}{\hbar} S_{\text{eff}}[\mathbf{n}^{(1)}, \mathbf{n}^{(2)}, z] = & M \sum_{i=1}^N \int dt \left\{ \frac{i}{\Gamma} \dot{\mathbf{n}}_i^{(1)}(t) \cdot \dot{\mathbf{n}}_i^{(2)}(t) + i \sum_{j=1}^N \mathcal{J}_{ij} \mathbf{n}_i^{(1)}(t) \cdot \mathbf{n}_j^{(2)}(t) \right. \\ & - \frac{1}{2} \int dt' \Sigma_B^K(t-t') \mathbf{n}_i^{(2)}(t) \cdot \mathbf{n}_i^{(2)}(t') + i \int dt' \Sigma_B^R(t-t') \mathbf{n}_i^{(2)}(t) \cdot \mathbf{n}_i^{(1)}(t') \\ & \left. - i z_i(t) \mathbf{n}_i^{(1)}(t) \cdot \mathbf{n}_i^{(2)}(t) \right\}, \end{aligned} \quad (5.33)$$

where introduced the real and symmetric matrix  $\mathcal{J}$  defined by  $\mathcal{J}_{ij} \equiv J_{ji}/\sqrt{N}$  if  $j < i$ ,  $\mathcal{J}_{ij} \equiv \mathcal{J}_{ji}$  if  $j > i$ . Like the other components of this matrix, we set  $\mathcal{J}_{ii}$  to be taken from a Gaussian distribution with zero mean and variance  $J^2/N$  [we saw that the constraint  $\mathbf{n}_i(t)^2 = 1$  yields  $\mathbf{n}_i^{(1)}(t) \cdot \mathbf{n}_i^{(2)}(t) = 0$ ]. The total effective action adopts the quadratic form

$$\frac{i}{\hbar} S_{\text{eff}} = -M \sum_{i=1}^N \int dt \left\{ i \mathbf{n}_i^{(2)}(t) \cdot \boldsymbol{\xi}_i(t) + \frac{1}{2} \int dt' \mathbf{n}_i^{(2)}(t) \cdot \Sigma_B^K(t-t') \mathbf{n}_i^{(2)}(t') \right\}, \quad (5.34)$$

where we introduced the  $N$  auxiliary fields  $\boldsymbol{\xi}_i$ :

$$\boldsymbol{\xi}_i(t) \equiv \sum_{j=1}^N \int dt' \left\{ \left[ \left( \frac{1}{\Gamma} \partial_t^2 + z_i(t) \right) \delta_{ij} - \mathcal{J}_{ij} \right] \delta(t-t') - \Sigma_B^R(t-t') \delta_{ij} \right\} \mathbf{n}_j^{(1)}(t'). \quad (5.35)$$

By integrating over  $\mathbf{n}_i^{(2)}$ , we are left with

$$\frac{i}{\hbar} S_{\text{eff}} = -M \sum_{i=1}^N \iint dt dt' \boldsymbol{\xi}_i(t) \cdot \frac{1}{2} \Sigma_B^{K-1}(t-t') \boldsymbol{\xi}_i(t'). \quad (5.36)$$

From this Gaussian action, the quantity  $\boldsymbol{\xi}_i(t)$  can be interpreted as a Gaussian random process with a zero average and variance  $\langle \boldsymbol{\xi}_i(t) \cdot \boldsymbol{\xi}_j(t') \rangle_\xi = \delta_{ij} \Sigma_B^K(t-t')$  and eq. (5.35) as a set of coupled Langevin equations. This mapping is possible since the action of the rotor system, once the constraint on each rotor has been imposed through  $z_i(t)$  and  $z_i(t)$  is treated independently, is quadratic. In more general models the mapping is not exact, see *e.g.* the discussion in [32].

Under the further assumption  $z_i(t) = z(t)$ , justified in the large  $M$  limit, the stochastic equations (5.35) are rendered independent – apart from a residual coupling through the Lagrange multiplier – by a rotation onto the basis that diagonalizes the interaction matrix  $\mathcal{J}$ . Indeed,  $\mathcal{J}$  being real and symmetric, it has  $N$  real eigenvalues  $J_\sigma$  with corresponding eigenvectors  $\boldsymbol{\sigma}$  that constitute a complete and orthonormal basis of the space of rotor sites:  $\boldsymbol{\sigma} \bullet \boldsymbol{\sigma}' = \delta_{\sigma\sigma'}$  where  $\bullet$  is the usual scalar product in this space. Let us collect all the rotors in the vector  $\mathbf{n} \equiv \{\mathbf{n}_i^{(1)}\}_{i \in [1, N]}$  and introduce its projections on the eigenvectors:  $\mathbf{n}_\sigma \equiv \mathbf{n} \bullet \boldsymbol{\sigma}$ . If we project eq. (5.35) onto  $\boldsymbol{\sigma}$ , we are left with  $N$  uncoupled Langevin equations reading

$$\left( \frac{1}{\Gamma} \partial_t^2 - J_\sigma + z(t) \right) \mathbf{n}_\sigma(t) - \int dt' \Sigma_B^R(t-t') \mathbf{n}_\sigma(t') = \boldsymbol{\xi}_\sigma(t), \quad (5.37)$$

with

$$\langle \boldsymbol{\xi}_\sigma(t) \rangle_\xi = 0, \quad \langle \boldsymbol{\xi}_\sigma(t) \cdot \boldsymbol{\xi}_{\sigma'}(t') \rangle_\xi = \delta_{\sigma\sigma'} \Sigma_B^K(t-t'). \quad (5.38)$$

The noise statistics is peculiar because of the quantum origin of the environment: it has memory (colored), and depends on  $T, eV, \hbar$ .

**Two-time self correlation.** Within the effective Langevin formalism, the two-time self correlation function defined in eq. (3.23) reads

$$C(t, t') = \overline{\langle \mathbf{n}_\sigma(t) \cdot \mathbf{n}_\sigma(t') \rangle}^J, \quad (5.39)$$

where the average over disorder is realized by

$$\overline{\cdots}^J \equiv \int dJ_\sigma \rho_J(J_\sigma) \cdots, \quad (5.40)$$

and  $\rho_J(J_\sigma)$  is the probability density of the eigenvalues of the interaction matrix  $\mathcal{J}$ . Following the analysis in [30], the correlation function (5.39) is expected to show a separation of time scales (at least in some parts of the phase diagram). This is usual in coarsening phenomena and corresponds to a stationary regime at short time-difference and an aging one at long time-difference with respect to a waiting-time dependent characteristic time. The stationary part of the correlation approaches a plateau at the Edwards-Anderson order parameter,  $q_{\text{EA}} \equiv \overline{\langle \mathbf{n}_\sigma \rangle_\xi^2}^J$ , that measures the fraction of frozen rotor fluctuations on time scales much smaller than this

characteristic time. The value of  $q_{\text{EA}}$  depends on all parameters  $(T, eV, \Gamma, g)$ . It is non-vanishing in the spontaneously symmetry-broken phase and continuously goes to 0 on the critical surface. In certain cases it can be computed exactly.

It is reasonable to expect that the long-time aging dynamics is determined by the low frequency (or long time) form of the Langevin equations only. The simplification arising in this asymptotic limit are discussed below.

### 5.5.3 Long-time dynamics

In the low-frequency, long time-difference limit,  $\hbar\omega \ll T$ , the Keldysh self-energy can be approximated by a constant [see, *e.g.*, eq. (4.20) in Sect. 4.2.3 for its exact expression in the  $\epsilon_F \rightarrow \infty$  limit]

$$\Sigma_B^K(\tau) \simeq \delta(\tau)\Sigma_B^K(\omega = 0) \geq 0. \quad (5.41)$$

Similarly, we keep the leading contributions in the derivative expansion of  $\Sigma_B^R$ :

$$\Sigma_B^R(\tau) \simeq \Sigma_B^R(\omega = 0)\delta(\tau) + \eta\delta(\tau)\partial_\tau, \quad (5.42)$$

with  $\eta \equiv \partial_\omega \text{Im} \Sigma_B^R(\omega = 0) > 0$ . The Langevin equations read in this limit

$$\frac{1}{\Gamma}\partial_t^2 \mathbf{n}_\sigma(t) + \eta\partial_t \mathbf{n}_\sigma(t) = (J_\sigma - z(t) + \Sigma_B^R(\omega = 0)) \mathbf{n}_\sigma(t) + \boldsymbol{\xi}_\sigma(t), \quad (5.43)$$

where  $\eta$  plays the role of a friction coefficient and  $\boldsymbol{\xi}_\sigma(t)$  has white noise statistics:

$$\langle \boldsymbol{\xi}_\sigma(t) \cdot \boldsymbol{\xi}_{\sigma'}(t') \rangle_\xi = \delta_{\sigma\sigma'} \delta(t - t') \Sigma_B^K(\omega = 0). \quad (5.44)$$

In the Langevin formalism, the kernel of an equilibrium white bath is given by the Einstein relation (known as the FDT of the second kind):  $\langle \xi(t)\xi(t') \rangle_\xi = 2\eta T \delta(t - t')$ . Thus, the temperature  $T$  of the bath can be seen as the ratio of the diffusion coefficient of a particle embedded in that bath with the friction coefficient  $\eta$  of the bath on the particle. For our reservoirs, in the low-frequency long time-difference limit, one can associate this ratio to an equivalent temperature  $T^*$

$$T^* \equiv \lim_{\omega \rightarrow 0} \frac{1}{2} \frac{\Sigma_B^K(\omega)}{\partial_\omega \text{Im} \Sigma_B^R(\omega)}, \quad (5.45)$$

the properties of which were discussed in Sect. 4.2.2. Thus, we confirm here that  $T^*$  acts like a temperature in the sense that the effect of the (out of equilibrium) reservoirs on the long-time dynamics is the one of an *equilibrium* dissipative (Ohmic) bath at a temperature  $T^*$ . This has been reported in different works and is at the root of the derivation of the stochastic Gilbert equation for a spin under bias [33].

We expect that as far as the long time dynamical behavior is concerned, the inertial term in eq. (5.43) can also be dropped, thus leading to the equations:

$$\partial_t \mathbf{n}_\sigma(t) = \lambda_\sigma(t) \mathbf{n}_\sigma(t) + \frac{1}{\eta} \boldsymbol{\xi}_\sigma(t), \quad (5.46)$$

where we introduced the shorthand notation  $\lambda_\sigma(t) \equiv [J_\sigma - \Delta z(t)]/\eta$  and  $\Delta z(t) \equiv z(t) - \Sigma_B^R(\omega = 0)$  and the spherical constraint is enforced by  $z(t)$ .

This particular Langevin equation has been analyzed intensively in the study of the classical spherical Sherrington-Kirkpatrick model (or spherical  $p = 2$  spin-glass model) and the results in [30] apply to our problem with  $T \mapsto T^*$ . The solution to eq. (5.46) for a given disorder realization and noise history is

$$\mathbf{n}_\sigma(t) = \mathbf{n}_\sigma(0) \exp\left(\int_0^t d\tau \lambda_\sigma(\tau)\right) + \frac{1}{\eta} \int_0^t d\tau \boldsymbol{\xi}_\sigma(\tau) \exp\left(\int_\tau^t d\tau' \lambda_\sigma(\tau')\right). \quad (5.47)$$

Copying results in [30], the aging part of the correlation (in the limit  $t' \gg t \rightarrow \infty$ ) shows a simple aging scaling behavior

$$C(t, t') \simeq 2\sqrt{2} q_{\text{EA}} \frac{(t/t')^{3/4}}{(1 + t/t')^{3/2}} = C(t/t'). \quad (5.48)$$

The solution to eqs. (5.46) leads to  $q_{\text{EA}} = 1 - T^*(eV, T)/J$ . However, this result is obtained by taking the limit of relatively close times – with respect to  $t'$  – whereas, as we stressed, eq. (5.46) is valid for the long time  $t'$  and long time-difference  $t - t'$  properties only. As a consequence, we expect the scaling result, eq. (5.48), to hold at long times with the value of the Edwards-Anderson parameter not necessarily given by  $1 - T^*(eV, T)/J$ . Its computation requires a full solution of the equations of motion.

We now focus on the aging dynamics in different parts of the phase diagram and argue that the Langevin dynamics of eq. (5.43) indeed provide a correct description of the dynamical evolution.

**Dynamics in the  $eV = 0$  plane.** In this case, the Edwards-Anderson order parameter  $q_{\text{EA}}$  measures the static order parameter. The dynamic calculations based on the use of the quantum FDT to relate the correlation to the linear response in the stationary regime detailed in [29], or the replica equilibrium computation in [35], can be easily extended to deal with a generic electronic bath in equilibrium. One confirms that  $q_{\text{EA}} = 1$  at  $T = \Gamma = eV = 0$  and continuously approaches 0 on the critical line  $\Gamma_c(T)$  for all values of  $g$ . The precise variation of  $q_{\text{EA}}$  within the coarsening phase depends on the bath kernels. In the  $\epsilon_F \rightarrow \infty$  limit, the results in [29] apply also to our problem. The solution of the Schwinger-Dyson equations in the aging regime confirms that the scaling result, eq. (5.48), holds.

**Dynamics in the  $\Gamma = 0$  plane.** Another interesting case is the effective overdamped Langevin limit obtained for  $\Gamma \rightarrow 0$  and  $(eV, T)$  in the coarsening phase. In this case dropping the inertial term in eq. (5.43) is exact and not an approximation.

Here the result  $q_{\text{EA}} = 1 - T^*(eV, T)/J$  can be shown to hold. The Edwards Anderson parameter approaches one for  $T = V = \Gamma = 0$  and goes continuously to zero on the critical line, as in a second order phase transition. Consistently with the analysis of the critical surface derived from the QNESS phase (see Sect. 5.4.2), one finds  $T^*(T_c, eV_c) = J$ . Numerical integration of the integro-differential equations of motion confirms that the scaling result, eq. (5.48), holds in the aging regime.

Despite the fact that dropping the inertial term is exact, the equations (5.46) are still not exact at all times. In particular, the initial conditions for this approximated equation of motion

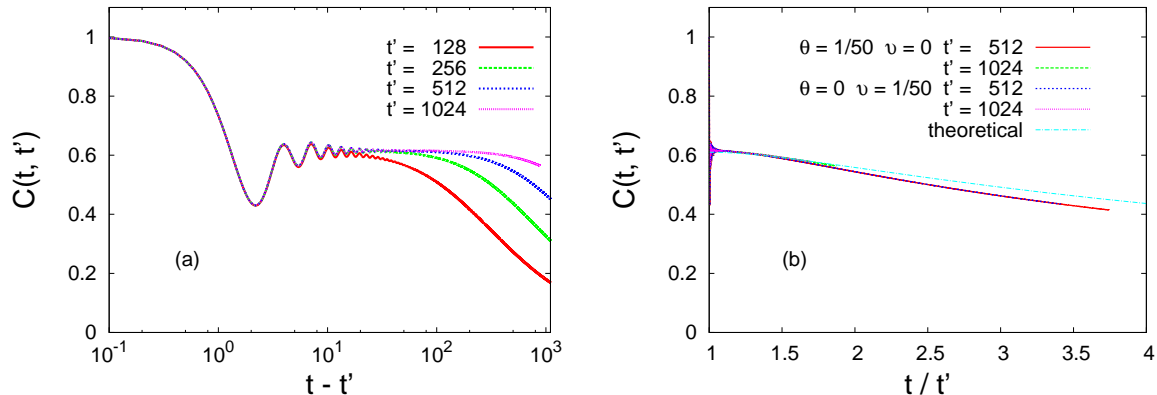


Figure 10: (Color online.) Dynamics in the driven coarsening regime: numerical solution to Schwinger-Dyson eqs. (5.6) and (5.7) where the reservoirs have a half-filled semi-circle DOS with  $\epsilon_F = 10J$ . (a) The self correlation  $C(t, t')$  after a quench to  $\theta = 0.02, v = 0.02, \gamma = 0.2, g = 1$  (in reduced quantities) shows first a stationary regime for short  $t - t'$ , then a slow aging regime where the time translational invariance is lost. (b) The self correlation  $C$  is plotted versus  $t/t'$  for two waiting times after two quenches into the coarsening region:  $\theta = 0.02, v = 0, \gamma = 0.2$  and  $\theta = 0, v = 0.02, \gamma = 0.2$ . There is a double collapse of the curves. The collapse for the different  $t'$  proves the simple aging scaling  $C(t'/t)$  and the collapse for the two different quenches shows that  $T^* \simeq eV/2$  plays the role of a temperature. The theoretical curve is the solution eq. (5.48) with  $q_{EA} \approx 0.6$ .

should be given by the state of the system a short while after the quench when the long-timescale description starts to be valid. Apparently, this delay seems to be not sufficient to significantly correlate the rotors with the interaction matrix  $\mathcal{J}$  and, to any practical purpose  $\mathbf{n}_\sigma(0)$  can still be considered “random”, at least as far as the Edwards-Anderson parameter is concerned.

**Dynamics in the  $T = 0$  plane.** The zero-temperature plane is more difficult to deal with analytically. One is not entitled to use FDT since the system is driven by  $eV$  nor dropping the second time-derivative is exact. Furthermore, this is the case where the simplification leading to eq. (5.46) are more dangerous because of the power law tails appearing at  $T = 0$  in correlation and response functions.

In order to check that the scaling result, eq. (5.48), holds we numerically integrate the full set of Schwinger-Dyson equations.

In Fig. 10 (a) we show the decay of the two-time correlation function. For short time differences  $t - t'$  with respect to the waiting time  $t'$ , there is a stationary regime depending on all control parameters in which the correlation approaches a plateau asymptotically in the time-difference. The plateau value is  $q_{EA}$  and measures the fraction of frozen rotor fluctuations on timescales much smaller than  $t'$ . Afterwards, there is an aging regime in which  $C$  depends on the two times explicitly. In Fig. 10 (b), we plot  $C$  against  $t/t'$  to prove that the simple aging scaling predicted analytically with eq. (5.48) holds at these long times. Moreover, we show that the dynamics after a quench to  $\theta = 0.2, v = 0$  are the same that the ones after a quench to  $\theta = 0, v = 0.2$ , illustrating the fact that  $T^* \simeq eV/2$  acts here like a temperature.

**Super-universality.** It is remarkable that in the large  $M$  limit, the long-time dynamics of our model are exactly the ones of the classical fully connected  $p = 2$  spherical spin glass. The

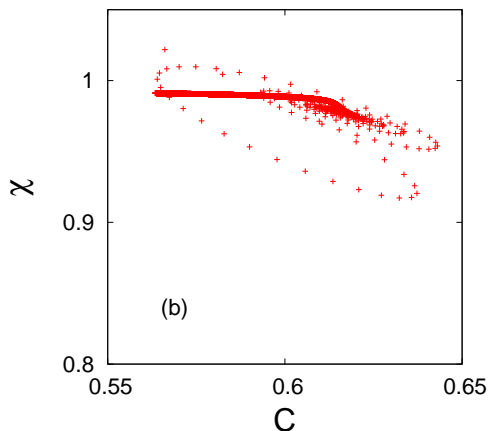


Figure 11: The integrated linear response,  $\chi(t, t') = \int_{t'}^t d\tau R(t, \tau)$  against  $C(t, t')$ , for  $t' = 1024$  and using  $t$  as a parameter. The curved part corresponds to the stationary and oscillatory regime with  $(t - t')/t' \rightarrow 0$  while the straight line is for times in the monotonic aging decay of  $C$ .

latter being a classical model in contact with an equilibrium bath ( $\Gamma = 0, eV = 0$ ), the former being its quantum version in contact with a non-equilibrium bath ( $\Gamma \neq 0, eV \neq 0$ ). The fact that the scaling functions are *super-universal*, in the sense that they do not depend on the external parameters  $T, eV, \Gamma$  once  $q_{\text{EA}}$  is extracted as a factor, can be understood as follows. First the fact that the non-equilibrium environment of our model gives rise to the same long-time dynamics than an equilibrium environment can be seen as a consequence of the Ohmic behavior of the reservoirs self-energy kernels at small frequencies (see Sect. 4.2.2). Second, the fact that our quantum model shows a classical behavior at late times can be understood as a consequence of decoherence due to the dissipative (and Ohmic) bath. Furthermore, the effect of the temperature  $T$  on the long-time dynamics being irrelevant (in a RG sense) in the classical limit, one can expect the same to hold in the quantum case with respect to all parameters.

This result has an interesting consequence. In the case of (large  $M$ ) quantum  $3d$  coarsening the classical-quantum mapping extends to space-time correlations and proves the existence of a growing coherence length  $R(t_w) \propto t_w^{1/2}$  over which the rotors are oriented in the same direction. This real-space interpretation of aging unveils the connection with coarsening that was announced all along this manuscript.

We found quite naturally that the long-time dynamics correspond to a Bose-Einstein-type condensation process of the  $N$   $M$ -dimensional “vectors”  $\mathbf{n}_\sigma$  on the direction of the edge eigenvector. The relaxation is controlled by the decay of  $\rho(J_\sigma)$  close to its edge. For Gaussian i.i.d. couplings  $\rho(J_\sigma) \propto [(2J)^2 - J_\sigma^2]^{1/2}$ . This coincides with the distribution of the modulus of the Laplacian eigenvalues,  $\rho(k^2) \propto (k^2)^{d/2-1}$  in  $d = 3$ . For this reason all models with a square root singularity of the distribution of “masses”  $J_\sigma$ , as the ferromagnetic rotor model in  $d = 3$  and the completely connected spin glass rotor model, are characterized by the same long-time dynamics.



### 5.5.4 Linear response

It has already been noticed in Sect. 5.2 that the response function was somehow peculiar since its equation of motion is decoupled from the one of the self correlation. Having argued that the long-time dynamics are governed by their classical counterparts, the linear response should also scale as in the classical limit. Therefore, the quantum fluctuation-dissipation relation between integrated linear response,  $\chi(t, t') \equiv \int_{t'}^t dt'' R(t, t'')$  and self correlation  $C(t, t')$  approaches the classical one,  $\chi \sim ct + (q_{\text{EA}} - C)/T_{\text{eff}}$ , with an *infinite* effective temperature [36],  $T_{\text{eff}} \rightarrow \infty$ , as shown in Fig. 11. The relations between integrated responses and correlation functions in other quantum problems that also approach classical-like form in the aging regime were shown in [31, 37].

### 5.5.5 The Lagrange multiplier

One should check the validity of a key assumption that was used to derive the phase diagram: the convergence of  $z(t)$  to an asymptotic value on the critical manifold. We first derive analytically the asymptotic behavior (within our long-time approximation) of  $z(t)$  in the  $\Gamma = 0$  coarsening phase showing that this is indeed the case. Then we give numerical evidence that  $z(t)$  converges in the whole phase space.

The condition  $C(t, t) = \int dJ_\sigma \rho_J(J_\sigma) \langle \mathbf{n}_\sigma(t) \cdot \mathbf{n}_\sigma(t) \rangle_\xi = 1$  reads after taking its time derivative and assuming furthermore that  $\mathbf{n}_\sigma(0)$  is uncorrelated with  $\sigma$  ( $\mathbf{n}_\sigma(0) = \mathbf{n}_0, \forall \sigma$ ), that is valid for random initial conditions (coming from infinite temperature for instance)

$$0 = \int dJ_\sigma \rho_J(J_\sigma) \langle \partial_t \mathbf{n}_\sigma(t) \cdot \mathbf{n}_\sigma(t) \rangle_\xi \quad (5.49)$$

$$= \int dJ_\sigma \rho_J(J_\sigma) \left\{ \mathbf{n}_0^2 \lambda_\sigma(t) e^{2 \int_0^t d\tau \lambda_\sigma(\tau)} + \frac{T^*}{\eta} \left[ 1 + 2\lambda_\sigma(t) \int_0^t d\tau' e^{2 \int_{\tau'}^t d\tau'' \lambda_\sigma(\tau'')} \right] \right\} \quad (5.50)$$

Taking the derivative with respect to  $\mathbf{n}_0^2$  yields

$$0 = \int dJ_\sigma \rho_J(J_\sigma) \lambda_\sigma(t) e^{2 \int_0^t d\tau \lambda_\sigma(\tau)}, \quad (5.51)$$

that can be recast into

$$\Delta z(t) = \frac{\eta}{2} \partial_t \ln \int dJ_\sigma \rho_J(J_\sigma) e^{2J_\sigma t / \eta}. \quad (5.52)$$

**Asymptotic behavior of  $z(t)$ .** By plugging the density of eigenvalues of an infinite ( $N \rightarrow \infty$ ) and symmetric random matrix with Gaussian elements of variance  $J^2/N$

$$\rho_J(J_\sigma) \equiv \frac{1}{\pi J} \sqrt{1 - \left( \frac{J_\sigma}{2J} \right)^2} \quad \text{for} \quad J_\sigma \in [-2J; +2J], \quad (5.53)$$

and zero elsewhere, we obtain

$$\Delta z(t) = \frac{\eta}{2} \partial_t \ln \frac{\eta}{2J} \frac{1}{t} I_1 \left( \frac{4J}{\eta} t \right), \quad (5.54)$$

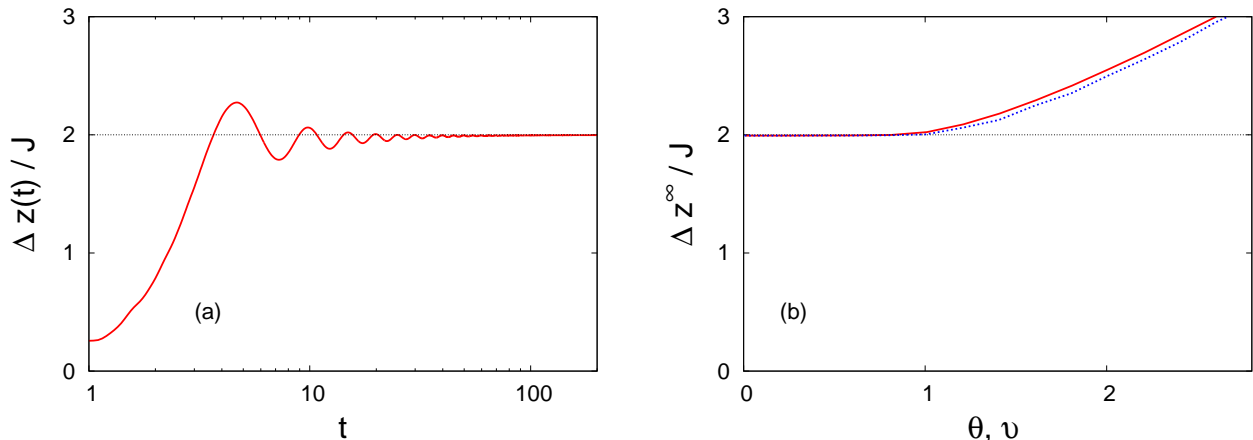


Figure 12: (Color online.) (a)  $\Delta z(t) \equiv z(t) - \Sigma_B^R(\omega = 0)$  quickly converges toward  $2J$ , the largest eigenvalue of the  $\mathcal{J}_{ij}$  matrix (here  $\Gamma = eV = T = 0.1J$ ,  $g = 1$ , and  $\epsilon_F = 10J$ ). (b) Dependence of  $z^\infty$  with  $T$  (plain curve) and  $eV$  (dashed curve).

where  $I_1$  is the modified Bessel function of the first kind and first order. We obtain, the pre-asymptotic behavior for  $t \gg \eta/J$

$$z(t) \simeq 2J + \Sigma_B^R(\omega = 0) - \eta \frac{3}{4t}. \quad (5.55)$$

We just showed that inside the coarsening phase, the Lagrange multiplier  $z(t)$  reaches an asymptotic value which is actually the critical value,  $z_c^\infty = 2J + \Sigma_B^R(\omega = 0)$ , calculated in Sect. 5.3 from the QNESS phase TTI equations without neglecting any term. The coherence between those two results somehow justifies the approximations made previously. In the  $\epsilon_F \rightarrow \infty$  limit (reservoirs acting like an Ohmic bath)  $\Sigma_R(\omega = 0)$  vanishes and we recover the same mechanism as in the classical case [30].

These analytical results are supported by the numerical analysis. Computed after the quench, the Lagrange multiplier  $z(t)$  quickly converges to an asymptotic value  $z^\infty$ . As an example, we plot in Fig. 12 (a) the behavior of  $z(t)$  after a quench into the QNESS phase. The oscillations and the zero initial slope are signatures of the second and higher order derivatives in eq. (5.37). These terms were dropped in the analytical study of the long-time limit, see eq. (5.46), but the numerical integration does not neglect them. We give in Fig. 12 (b) the dependence of  $z^\infty$  with  $T$  and  $eV$ . It is quite clear that  $z^\infty$  is constant (and equal to  $z_c^\infty$ ) inside the critical surface and increases with  $T$ ,  $\Gamma$ , and  $eV$  as soon as entering the QNESS phase. This justifies the assumptions made in Sect. 5.3.

To summarize the results, in the whole phase diagram  $z(t)$  always rapidly reaches an asymptotic value  $z^\infty$ . Inside the QNESS phase,  $z^\infty$  is a growing function of the parameters  $T, \Gamma, V$  whereas on the critical surface and inside the coarsening region, it is fixed to  $z_c^\infty$ .

**Link between  $z(t)$  and the potential energy density** One is interested in computing the energy density  $\epsilon(t)$  of the effective Brownian particle. It is given by

$$\epsilon(t) = -\frac{1}{2} \sum_{i,j=1}^N \overline{J_{ij} \mathbf{n}_i(t) \mathbf{n}_j(t)}^J = -\frac{1}{2} \int dJ_\sigma \rho_J(J_\sigma) J_\sigma \mathbf{n}_\sigma^2(t) . \quad (5.56)$$

Using the solution (5.47) for  $\mathbf{n}_\sigma(t)$  at  $T^* = 0$ , one has

$$2\epsilon(t) = -\mathbf{n}_0^2 e^{-\frac{2}{\eta} \int_0^t d\tau \Delta z(\tau)} \int dJ_\sigma J_\sigma \rho(J_\sigma) e^{2J_\sigma t/\eta} . \quad (5.57)$$

By use of eq. (5.52), we obtain

$$2\epsilon(t) = -\frac{\eta}{2} \partial_t \ln \int dJ_\sigma \rho(J_\sigma) e^{2J_\sigma t/\eta} . \quad (5.58)$$

We recognize eq. (5.52) in the right-hand-side (RHS) of this last expression, giving finally

$$\epsilon(t) = -\frac{1}{2} \Delta z(t) . \quad (5.59)$$

This result is valid for any disorder density  $\rho(J_\sigma)$ . For a non-zero  $T^*$ , similar calculations give, see [30],

$$\epsilon(t) = \frac{1}{2} [T^* - \Delta z(t)] . \quad (5.60)$$

## 6 The current

The physics of electric currents through mesoscopic quantum impurities in out-of-equilibrium settings has attracted a lot of attention in the recent years. The Kondo impurity is the canonical example of a strongly correlated system that has both been tackled experimentally [41] and theoretically by non-perturbative methods [42]. It is, to our knowledge, the first time that some fermionic reservoirs are coupled to a macroscopic disordered quantum system. In the previous Sections we analyzed the effects of the voltage drop on the system dynamics. In this Section we study the properties of the current that establishes between the two reservoirs. In particular we are interested in the possible influence of the rotors on the current. Is the current, that is rather easy to measure experimentally, able to give information about the dynamics of the rotors ?

We recall the expression of the interaction Hamiltonian given in eq. (2.8):

$$H_{SB} = -\sqrt{M} \frac{\hbar\omega_c}{N_s} \sum_{i=1}^N \sum_{\mu=1}^M \sum_{k,k'=1}^{N_s} \sum_{l,l'=1}^{\mathcal{M}} n_i^\mu [\psi_{Likl}^\dagger \sigma_{ll'}^\mu \psi_{Rik'l'} + L \leftrightarrow R] . \quad (6.1)$$

From the point of view of the electric current, our model consists in two reservoirs coupled through time-dependent tunneling constants  $n_i^\mu(t)$ . It is different from the usual quantum

impurity problems in the fact that the electrons cannot stay on the rotor system but only hop directly from one reservoir to the other. Furthermore, the quantum character of the system is not expected to play any significant role since its level spacings are smaller than any other energy scale in the large  $MN$  limit. The computation of the current will therefore lead to Landauer formula [43] *a priori* dependent on the rotors states.

The electric current carried by the fermions flowing from the right to the left reservoirs is

$$I_{R \rightarrow L}(t) = -e \left\langle \frac{dN_L}{dt} \right\rangle = -\frac{ie}{\hbar} \langle [H, N_L] \rangle = -\frac{ie}{\hbar} \langle [H_{SB}, N_L] \rangle, \quad (6.2)$$

where  $-e$  is the electric charge of a fermion and  $N_L \equiv \sum_{ikl} \psi_{Likl}^\dagger \psi_{Likl}$  is the number operator of the left reservoirs.  $H_{SB}$  is the part of the total Hamiltonian  $H$  that couples the system and the reservoirs, see eq. (2.8). After straightforward algebra, we obtain

$$I_{R \rightarrow L}(t) = -\frac{ie}{\hbar} \langle \sqrt{M} \frac{\hbar\omega_c}{N_s} \sum_{i\mu k k' l l'} \sigma_{ll'}^\mu n_i^\mu [\psi_{Likl}^\dagger \psi_{Rjk'l'} - L \leftrightarrow R] \rangle. \quad (6.3)$$

In the Keldysh field theory formalism, this corresponds to the quantity

$$I_{R \rightarrow L}(t) = \frac{1}{2} (I_{R \rightarrow L}^+(t) + I_{R \rightarrow L}^-(t)), \quad (6.4)$$

with

$$I_{R \rightarrow L}^a(t) \equiv -\frac{ie}{\hbar} \langle \sqrt{M} \frac{\hbar\omega_c}{N_s} \sum_{i\mu k k' l l'} \sigma_{ll'}^\mu n_i^{\mu a}(t) [\bar{\psi}_{Likl}^a(t) \psi_{Rjk'l'}^a(t) - L \leftrightarrow R] \rangle. \quad (6.5)$$

Expanding the action up to first order in the coupling constant  $g$ , we obtain an average over the rotors and the free fermions that are now uncoupled, that we note  $\langle \cdots \rangle_{SB}$

$$\begin{aligned} I_{R \rightarrow L}(t) &= \frac{1}{2} \langle (I_{L \rightarrow R}^+(t) + I_{L \rightarrow R}^-(t)) \frac{i}{\hbar} S_{SB} \rangle_{SB} \\ &= \frac{e}{2\hbar^2} M \left( \frac{\hbar\omega_c}{N_s} \right)^2 \sum_{ab} \sum_{i\mu k k' l l' j\nu q q' m m'} \sum_b \int dt' \sigma_{ll'}^\mu \sigma_{mm'}^\nu \langle n_i^{\mu a}(t) n_j^{\nu b}(t') \rangle \\ &\quad \times [\bar{\psi}_{Likl}^a(t) \psi_{Rjk'l'}^a(t) - L \leftrightarrow R] [\bar{\psi}_{Ljqm}^b(t') \psi_{Rjq'm'}^b(t') + L \leftrightarrow R] \rangle_{SB}. \end{aligned} \quad (6.6)$$

Averaging over the free fermions, we obtain

$$I_{R \rightarrow L}(t) = \frac{e}{2\hbar^2} MN (\hbar\omega_c)^2 \sum_{ab=\pm} b \int dt' i\hbar G^{ab}(t, t') [i\hbar G_L^{ab}(t, t') i\hbar G_R^{ba}(t', t) - L \leftrightarrow R]. \quad (6.7)$$

$G^{ab}$  are the macroscopic Keldysh Green's functions for the rotors and  $G_{L/R}^{ab}$  are the Green's functions of the free fermions in the  $L/R$ -reservoirs. This reads, after Keldysh rotations,

$$I_{R \rightarrow L}(t) = -\frac{e}{\hbar} MN \int_0^t d\tau C(t, t-\tau) \Pi_B^R(\tau) + R(t, t-\tau) \Pi_B^K(\tau), \quad (6.8)$$

with

$$\begin{aligned}\Pi_B^K &\equiv -2(\hbar\omega_c)^2 \operatorname{Im} \left[ G_L^K G_R^{K*} - \frac{\hbar^2}{4} (G_L^R G_R^{R*} + G_L^A G_R^{A*}) \right], \\ \Pi_B^R &\equiv -2(\hbar\omega_c)^2 \operatorname{Im} \left[ G_L^R G_R^{K*} + G_L^K G_R^{R*} \right].\end{aligned}\quad (6.9)$$

The expression for the current given in eq. (6.8) is quite generic. It is valid as soon as the system and the fermionic leads are coupled with an interaction  $H_{SB}$ . The details of the system and the leads enter in the formula through their respective Green's functions. The formula was obtained after a first order expansion in the coupling constant  $g$ . The second order term like all the even order terms are zero by use of Wick's theorem. The third and higher odd order terms would have involved higher order correlation functions of the system. Plugging the expressions of the fermionic Green's functions  $G_\alpha^K$ ,  $G_\alpha^R$ , and  $G_\alpha^A$  ( $\alpha = L, R$ ) that are given in Appendix B.1, we get

$$\Pi_B^K(\tau) = \frac{1}{2}(\hbar\omega_c)^2 \langle\langle \left[ \tanh\left(\beta\frac{\epsilon_L - \mu_L}{2}\right) \tanh\left(\beta\frac{\epsilon_R - \mu_R}{2}\right) - 1 \right] \sin\left(\frac{\epsilon_L - \epsilon_R}{\hbar}\tau\right) \rangle\rangle_{L,R}, \quad (6.10)$$

$$\Pi_B^R(\tau) = \frac{1}{\hbar}(\hbar\omega_c)^2 \langle\langle \left[ \tanh\left(\beta\frac{\epsilon_L - \mu_L}{2}\right) - \tanh\left(\beta\frac{\epsilon_R - \mu_R}{2}\right) \right] \cos\left(\frac{\epsilon_L - \epsilon_R}{\hbar}\tau\right) \rangle\rangle_{L,R} \Theta(\tau), \quad (6.11)$$

where the notation  $\langle\langle \dots \rangle\rangle_{L,R}$  stands for  $\iint d\epsilon d\epsilon' \rho_L(\epsilon) \rho_R(\epsilon') \dots$ . One can check that the current vanishes when the bias voltage ( $eV \equiv \mu_R - \mu_L$ ) is set to zero.

**Linear conductance.** We develop the current formula (6.8) to the first order in  $eV$  and compute the linear conductance

$$I_{R \rightarrow L}(t) = -\frac{e}{\hbar} MN eV \int_0^t d\tau \left. C(t, t - \tau) \right|_{eV=0} + \left. R(t, t - \tau) \right|_{eV=0} \frac{d\Pi_B^K(\tau)}{deV} \Big|_{eV=0}, \quad (6.12)$$

One can derive for a flat half-filled DOS,  $\rho(\epsilon) \propto \Theta(\epsilon_F - |\epsilon - \epsilon_F|)$ , in the limit  $\epsilon_F \rightarrow \infty$  (in that limit we expect the results to depend very little on the precise shape of the DOS)

$$\left. \frac{d\Pi_B^R(\tau)}{deV} \right|_{eV=0} = -\pi g^2 \delta(\tau), \quad (6.13)$$

$$\left. \frac{d\Pi_B^K(\tau)}{deV} \right|_{eV=0} = -\hbar g^2 \frac{1}{2\tau}. \quad (6.14)$$

Therefore the linear current very quickly goes from zero to

$$I_{R \rightarrow L}(t) = \frac{e}{2\hbar} MN g^2 eV \left( \pi + \hbar \int_0^t d\tau \frac{R(t, t - \tau)}{\tau} \right). \quad (6.15)$$

The dependence on the history of the two-time correlation function has disappeared and the second term in eq. (6.15) goes to zero due to the rapid decay of the response function. Finally the current quickly takes an asymptotic value

$$I_{R \rightarrow L}^\infty = \frac{e}{2\hbar} \pi MN g^2 eV. \quad (6.16)$$

From this computation, it appears that the current only probes the very fast dynamics of the system it passes through and does not give information on the long-time dynamics. Since the short-time dynamics of the system are equilibrium ones even in the coarsening regime, the current cannot be used to tell in which regime the system is. An exact numerical integration of eq. (6.8) supports these findings for other types of DOS, for finite values of  $\epsilon_F$  and far from the linear regime.

## 7 Conclusions and discussion

In this paper we presented a detailed study of the quantum fully-connected rotor model driven out of equilibrium by a fermionic drive. We determined analytically the phase diagram of the model and we showed that a critical manifold, controlled by the value of the disorder strength, separates a QNESS with zero order parameter from an ordering phase with non-zero order parameter. We solved the equations that describe the dynamics in the different phases with a numerical integration and analytically by using various approximation schemes that give valuable physical insights. In particular, we showed that this (quasi) quadratic model maps to a set of Langevin equations with additive colored noise that describes the dynamics of the rotors. The nature of the noise is determined by the type of electron baths used and, in the driven case, the friction kernel and noise-noise correlation are not linked by any fluctuation-dissipation relation. By using this effective Langevin description we established the connection with the  $3d$  coarsening dynamics of the  $\mathcal{O}(M)$  model and we showed that the long-time ordering dynamics are in the class of the classical limit of our model without a drive, *i.e.*, with the typical length growing as  $t^{1/2}$ .

Finally, we derived a generic expression for the current flowing through the system that involves a time-convolution between the characteristics of the system (through its correlation and linear response) and the ones the leads (through their retarded and Keldysh kernels). Interestingly enough, for the type of density of states used in the large  $\epsilon_F$  limit the current depends only on the short-time difference (stationary) regime in which coarsening is not relevant.

Future studies along these lines include the analysis of the fate of first order phase transitions, common in disordered quantum spin systems with multi-spin interactions when driven out of equilibrium.

## 8 Acknowledgments

We thank C. Chamon, L. Chaput, A. Millis and A. Mitra for useful discussions. This work was financially supported by ANR-BLAN-0346 (FAMOUS).

# Appendices

## A Conventions

$\Theta$  is the Heaviside step function. We choose  $\Theta(0) = 1/2$ , so that  $\Theta(x) + \Theta(-x) = 1 \forall x \in \mathbb{R}$ . We recall the identities

$$\int_{-\infty}^{\infty} \frac{dx}{2\pi} e^{ixy} = \delta(y) \quad \text{and} \quad \int_{-\infty}^y dx \delta(x) = \Theta(y), \quad (\text{A.1})$$

where  $\delta$  is the Dirac delta function. In particular  $\int_{-\infty}^0 dx \delta(x) = 1/2$ .

### A.1 Fourier transform

The convention for the Fourier transform  $\mathcal{F}$  that we use is

$$\begin{aligned} \mathcal{F}[f(\tau)](\omega) &\equiv f(\omega) \equiv \int_{-\infty}^{\infty} d\tau e^{+i\omega\tau} f(\tau), \\ \mathcal{F}^{-1}[f(\omega)](\tau) &\equiv f(\tau) = \int_{-\infty}^{\infty} \frac{d\omega}{2\pi} e^{-i\omega\tau} f(\omega), \end{aligned} \quad (\text{A.2})$$

The Fourier transform of the step function is

$$\mathcal{F}[\Theta(\tau)](\omega) = i \text{pv} \frac{1}{\omega} + \pi\delta(\omega), \quad (\text{A.3})$$

where ‘pv’ denotes the principal value. Convolutions in real and Fourier spaces are defined by

$$\begin{aligned} (f \circ g)(\tau) &\equiv \int d\tau' f(\tau')g(\tau - \tau') = \mathcal{F}^{-1}[(f g)(\omega)](\tau), \\ (f \circ g)(\omega) &\equiv \int \frac{d\omega'}{2\pi} f(\omega')g(\omega - \omega') = \mathcal{F}[(f g)(\tau)](\omega). \end{aligned} \quad (\text{A.4})$$

### A.2 Heisenberg representation

In the Heisenberg representation the operators evolve as

$$A_H(t) = U^\dagger(t)A(t)U(t). \quad (\text{A.5})$$

with the unitary operator

$$U(t) \equiv \mathbb{T} e^{-\frac{i}{\hbar} \int_0^t dt' H(t')}, \quad (\text{A.6})$$

and thus  $U^\dagger(t) = \tilde{\mathbb{T}} e^{-\frac{i}{\hbar} \int_t^0 dt' H(t')}$ .  $\mathbb{T}$  and  $\tilde{\mathbb{T}}$  are respectively the time and anti-time-ordering operators (see Appendix A.3). For Hamiltonians  $H$  that do not explicitly depend on time we get

$$A_H(t) = e^{iHt/\hbar} A(t) e^{-iHt/\hbar}. \quad (\text{A.7})$$

### A.3 Time-ordering operator

On the real time axis, the time-ordering operator  $\mathbb{T}$  rearranges operators with ascending times to the left:

$$\mathbb{T} A_{\text{H}}(t)B_{\text{H}}(t') = A_{\text{H}}(t)B_{\text{H}}(t')\Theta(t-t') + \zeta B_{\text{H}}(t')A_{\text{H}}(t)\Theta(t'-t), \quad (\text{A.8})$$

with  $\zeta = -1$  if both  $A$  and  $B$  are fermionic operators,  $\zeta = 1$  otherwise. The anti-time-ordering operator  $\tilde{\mathbb{T}}$  rearranges operators the other way round:

$$\tilde{\mathbb{T}} A_{\text{H}}(t)B_{\text{H}}(t') = A_{\text{H}}(t)B_{\text{H}}(t')\Theta(t'-t) + \zeta B_{\text{H}}(t')A_{\text{H}}(t)\Theta(t-t'), \quad (\text{A.9})$$

On the Keldysh contour  $\mathcal{C}$ , the position of an operator is specified by both the time and the branch index. By the notation  $A_{\text{H}}(t, a)$ , we denote the operator  $A$  in the Heisenberg representation at time  $t$  ( $t \in [0, +\infty[$ ) on the branch  $a$  ( $a = \pm$ ). One can similarly define a time-ordering operator  $\mathbb{T}_{\mathcal{C}}$  that rearranges operators along the contour  $\mathcal{C}$  represented in Fig. 5. The rules are

$$\begin{aligned} \mathbb{T}_{\mathcal{C}} A_{\text{H}}(t, -)B_{\text{H}}(t', +) &= A_{\text{H}}(t)B_{\text{H}}(t'), \\ \mathbb{T}_{\mathcal{C}} A_{\text{H}}(t, +)B_{\text{H}}(t', -) &= \zeta B_{\text{H}}(t')A_{\text{H}}(t), \\ \mathbb{T}_{\mathcal{C}} A_{\text{H}}(t, +)B_{\text{H}}(t', +) &= A_{\text{H}}(t)B_{\text{H}}(t')\Theta(t-t') + \zeta B_{\text{H}}(t')A_{\text{H}}(t)\Theta(t'-t), \\ \mathbb{T}_{\mathcal{C}} A_{\text{H}}(t, -)B_{\text{H}}(t', -) &= A_{\text{H}}(t)B_{\text{H}}(t')\Theta(t'-t) + \zeta B_{\text{H}}(t')A_{\text{H}}(t)\Theta(t-t'). \end{aligned} \quad (\text{A.10})$$

### A.4 Green's functions

Let  $\phi$  and  $\phi^\dagger$  be respectively annihilation and creation operators (bosonic or fermionic). In the field theory formalism of the Keldysh approach, we define the Green's functions as

$$i\hbar G^{ab}(t, t') \equiv \langle \phi^a(t)\bar{\phi}^b(t') \rangle. \quad (\text{A.11})$$

$a, b = \pm$ ,  $\bar{\phi}$  is either the complex conjugate (for bosons) or the Grassmannian conjugate (for fermions) of  $\phi$  and the average is understood as

$$\langle \dots \rangle \equiv \int \mathcal{D}[\phi^\pm, \bar{\phi}^\pm] \dots \exp\left(\frac{i}{\hbar} S[\phi^\pm, \bar{\phi}^\pm]\right). \quad (\text{A.12})$$

In the operator formalism the Green's function read

$$i\hbar G^{ab}(t, t') \equiv \text{Tr} \left[ \mathbb{T}_{\mathcal{C}} \phi_{\text{H}}(t, a) \phi_{\text{H}}^\dagger(t', b) \varrho_{\text{H}}(0, \pm) \right], \quad (\text{A.13})$$

where  $\phi_{\text{H}}(t, a)$  denotes the Heisenberg representation of the operator  $\phi$  at time  $t$  on the  $a$ -branch of the Keldysh contour.  $\varrho_{\text{H}}(0, \pm) = \varrho(0)$  is the initial density matrix (normalized to be of unit trace) and its location on the  $+$  or  $-$ -branch does not matter thanks to the cyclicity of the trace.  $\mathbb{T}_{\mathcal{C}}$  is the time-ordering operator acting with respect to the relative position of  $(t, a)$  and  $(t', b)$  on the Keldysh contour (see Appendix A.3).

One has, independently of the bosonicity or fermonicity of the field

$$G^{ab}(t', t) = -G^{\bar{b}\bar{a}}(t, t')^*, \quad (\text{A.14})$$

where the star indicates complex conjugate and  $\bar{a} \equiv -a$ .



## B Fermionic bath

We define the fermionic Keldysh Green's functions

$$i\hbar G^{ab}(t, t') \equiv \langle \psi^a(t) \bar{\psi}^b(t') \rangle, \quad (\text{B.1})$$

where  $a, b = \pm$ . Like for bosons [see eqs. (3.21)], one has

$$\begin{aligned} G^{++}(t, t') &= G^{-+}(t, t')\Theta(t - t') + G^{+-}(t, t')\Theta(t' - t), \\ G^{--}(t, t') &= G^{+-}(t, t')\Theta(t - t') + G^{-+}(t, t')\Theta(t' - t), \end{aligned} \quad (\text{B.2})$$

leading to the relation between Keldysh Green's functions

$$G^{++} + G^{--} = G^{+-} + G^{-+}. \quad (\text{B.3})$$

### B.1 Keldysh rotation

We introduce the new fermionic fields

$$\begin{cases} 2\psi^{(1)} \equiv \psi^+ + \psi^-, & 2\bar{\psi}^{(1)} \equiv \bar{\psi}^+ + \bar{\psi}^-, \\ \hbar\psi^{(2)} \equiv \psi^+ - \psi^-, & \hbar\bar{\psi}^{(2)} \equiv \bar{\psi}^+ - \bar{\psi}^-. \end{cases} \quad (\text{B.4})$$

These definitions leads to

$$\begin{aligned} i\hbar G^{(11)}(t, t') &\equiv \langle \psi^{(1)}(t) \bar{\psi}^{(1)}(t') \rangle = i\hbar/4 [G^{++} + G^{--} + G^{-+} + G^{+-}] \equiv G^K, \\ i\hbar G^{(12)}(t, t') &\equiv \langle \psi^{(1)}(t) \bar{\psi}^{(2)}(t') \rangle = i/2 [G^{++} - G^{--} + G^{-+} - G^{+-}] \equiv -iG^R, \\ i\hbar G^{(21)}(t, t') &\equiv \langle \psi^{(2)}(t) \bar{\psi}^{(1)}(t') \rangle = i/2 [G^{++} - G^{--} - G^{-+} + G^{+-}] \equiv iG^A, \\ i\hbar G^{(22)}(t, t') &\equiv \langle \psi^{(2)}(t) \bar{\psi}^{(2)}(t') \rangle = i/\hbar [G^{++} + G^{--} - G^{-+} - G^{+-}] = 0. \end{aligned} \quad (\text{B.5})$$

Where we defined, *en passant*, the Keldysh  $G^K$ , the retarded  $G^R$  and the advanced  $G^A$  Green's functions in the same manner that we did for  $C$  and  $R$  in Sect. 3.3.4. Using relation (B.3) we get

$$G^K = i\hbar/2 [G^{++} + G^{--}] = i\hbar/2 [G^{+-} + G^{-+}], \quad (\text{B.6})$$

$$G^R = -[G^{++} - G^{+-}] = [G^{+-} - G^{-+}] \Theta(\tau), \quad (\text{B.7})$$

$$G^A = [G^{++} - G^{-+}] = [G^{+-} - G^{-+}] \Theta(-\tau), \quad (\text{B.8})$$

which are inverted as

$$i\hbar G^{ab} = G^K + \frac{i\hbar}{2}(a G^A - b G^R). \quad (\text{B.9})$$

### B.2 Symmetry properties under $t \leftrightarrow t'$

Using eq. (A.14), one establishes

$$G^R(\tau) = -G^A(-\tau)^*, \quad G^K(\tau) = G^K(-\tau)^*. \quad (\text{B.10})$$

And hence in Fourier space

$$G^R(\omega) = -G^A(\omega)^*, \quad G^K(\omega) \in \mathbb{R}. \quad (\text{B.11})$$

## B.3 Free fermions

### B.3.1 Single free fermion

The free fermion Hamiltonian is

$$H = \epsilon \psi^\dagger \psi . \quad (\text{B.12})$$

Starting from the expression in terms of operators of the Keldysh Green's functions,

$$i\hbar G^{ab}(t, t') = \text{Tr} \left[ \mathbb{T}_C \psi_H(t, a) \psi_H^\dagger(t', b) \varrho(0) \right] , \quad (\text{B.13})$$

with  $a, b = \pm$  and the grand-canonical density matrix  $\varrho(0) \propto e^{-\beta(H - \mu N)}$ , one computes

$$\begin{aligned} i\hbar G^{+-}(\epsilon; \tau) &= -n_F e^{-\frac{i}{\hbar}\epsilon\tau} , \\ i\hbar G^{-+}(\epsilon; \tau) &= (1 - n_F) e^{-\frac{i}{\hbar}\epsilon\tau} . \end{aligned} \quad (\text{B.14})$$

$n_F$  is the Fermi factor given by  $n_F(\epsilon) \equiv (1 + e^{\beta(\epsilon - \mu)})^{-1}$ . After the Keldysh rotation we get

$$\begin{aligned} G^K(\epsilon; \tau) &= \frac{1}{2} \tanh\left(\beta \frac{\epsilon - \mu}{2}\right) e^{-\frac{i}{\hbar}\epsilon\tau} , \\ G^R(\epsilon; \tau) &= \frac{i}{\hbar} e^{-\frac{i}{\hbar}\epsilon\tau} \Theta(\tau) , \\ G^A(\epsilon; \tau) &= \frac{i}{\hbar} e^{-\frac{i}{\hbar}\epsilon\tau} \Theta(-\tau) . \end{aligned} \quad (\text{B.15})$$

### B.3.2 Collection of free fermions

For our left and right reservoirs, we consider continuous distribution (density of states)  $\rho_L(\epsilon)$  and  $\rho_R(\epsilon)$  of these free fermions. This yields to the Keldysh Green's functions

$$G_\alpha^{ab}(\tau) = \int d\epsilon \rho_\alpha(\epsilon) G_\alpha^{ab}(\epsilon; \tau) , \quad (\text{B.16})$$

with  $\alpha = L, R$ . After a Keldysh rotation it yields

$$\begin{aligned} G^K(\tau) &= \int d\epsilon \rho(\epsilon) \frac{1}{2} \tanh[\beta(\epsilon - \mu)/2] e^{-\frac{i}{\hbar}\epsilon\tau} = \frac{1}{2} \langle \tanh[\beta(\epsilon - \mu)/2] e^{-\frac{i}{\hbar}\epsilon\tau} \rangle_\epsilon , \\ G^R(\tau) &= \int d\epsilon \rho(\epsilon) \frac{i}{\hbar} e^{-\frac{i}{\hbar}\epsilon\tau} \Theta(\tau) = \frac{i}{\hbar} \langle e^{-\frac{i}{\hbar}\epsilon\tau} \rangle_\epsilon \Theta(\tau) , \\ G^A(\tau) &= \int d\epsilon \rho(\epsilon) \frac{i}{\hbar} e^{-\frac{i}{\hbar}\epsilon\tau} \Theta(-\tau) = \frac{i}{\hbar} \langle e^{-\frac{i}{\hbar}\epsilon\tau} \rangle_\epsilon \Theta(-\tau) , \end{aligned} \quad (\text{B.17})$$

where we introduced a short-hand notation for the integration over energy levels. In terms of the Fourier transforms of  $\rho(\epsilon)$  it reads

$$G^R(\tau) = \frac{i}{\hbar} 2\pi \rho(\tau/\hbar) \Theta(\tau) , \quad G^A(\tau) = \frac{i}{\hbar} 2\pi \rho(\tau/\hbar) \Theta(-\tau) . \quad (\text{B.18})$$

### B.3.3 Fourier transforms

$$\begin{aligned} G^K(\omega) &= \pi\hbar \tanh\left(\beta\frac{\hbar\omega - \mu}{2}\right) \rho(\hbar\omega) \in \mathbb{R} , \\ G^R(\omega) + G^A(\omega) &= 2i\pi\rho(\hbar\omega) \in i\mathbb{R} . \end{aligned} \tag{B.19}$$

Since  $\rho(\epsilon)$  is real, one computes

$$\text{Im}G^R(\omega) = \pi\rho(\hbar\omega) . \tag{B.20}$$

Thus we get, as a check, the grand-canonical fermionic fluctuation-dissipation theorem that is established generally in Sect. C:

$$G^K(\omega) = \hbar \tanh\left(\beta\frac{\hbar\omega - \mu}{2}\right) \text{Im} G^R(\omega) . \tag{B.21}$$

## C Fluctuation-Dissipation Theorem

In this Section we give a proof of the fluctuation-dissipation theorem both in its bosonic and fermionic versions. This theorem only holds in equilibrium and gives a relation between the Green's functions. In the grand-canonical ensemble, the initial density operator reads  $\varrho(0) \propto \exp(-\beta(H - \mu N))$ , where  $N$  is the number operator commuting with  $H$  (in non-relativistic quantum mechanics),  $\mu$  is the chemical potential fixing the average number of particles. One can obtain the theorem for the canonical ensemble by formally setting  $\mu = 0$ . Let us consider a pair of either bosonic or fermionic operators, for instance creation and annihilation operators  $\phi^\dagger$  and  $\phi$ . Let us write the following Keldysh Green's function

$$i\hbar G^{+-}(t, t') = \text{Tr} \left[ \mathbb{T}_c \phi_{\text{H}}(t, +) \phi_{\text{H}}^\dagger(t', -) \varrho(0) \right] . \tag{C.1}$$

By resolving the time-ordering we get

$$i\hbar G^{+-}(t, t') = \zeta \text{Tr} \left[ \phi_{\text{H}}^\dagger(t') \phi_{\text{H}}(t) \varrho(0) \right] , \tag{C.2}$$

with  $\zeta = +1$  in the bosonic case and  $\zeta = -1$  in the fermionic case. Using the *analyticity* of the Green's functions and then expanding  $\phi_{\text{H}}(t + i\beta\hbar) = \exp(-\beta H) \phi_{\text{H}}(t) \exp(+\beta H)$ , we get

$$i\hbar G^{+-}(t + i\beta\hbar, t') = \zeta \text{Tr} \left[ \phi_{\text{H}}^\dagger(t') \phi_{\text{H}}(t + i\beta\hbar) \varrho(0) \right] \tag{C.3}$$

$$\propto \zeta \text{Tr} \left[ \phi_{\text{H}}^\dagger(t') \exp(-\beta H) \phi_{\text{H}}(t) \exp(\beta\mu N) \right] . \tag{C.4}$$

Since  $H$  and  $N$  commute and since for any operator  $f(N)$ , one has  $\phi f(N) = f(N + 1)\phi$ , we have

$$\phi_{\text{H}}(t) \exp(\beta\mu N) = \exp(\beta\mu(N + 1)) \phi_{\text{H}}(t) , \tag{C.5}$$

and so

$$i\hbar G^{+-}(t + i\beta\hbar, t') = \zeta \exp(\beta\mu) \text{Tr} \left[ \phi_{\text{H}}^\dagger(t') \varrho(0) \phi_{\text{H}}(t) \right]. \quad (\text{C.6})$$

Using the *cyclicity* of the trace, we come to

$$i\hbar G^{+-}(t + i\beta\hbar, t') = \zeta \exp(\beta\mu) \text{Tr} \left[ \phi_{\text{H}}(t) \phi_{\text{H}}^\dagger(t') \varrho(0) \right] \quad (\text{C.7})$$

$$= \zeta \exp(\beta\mu) i\hbar G^{-+}(t, t'). \quad (\text{C.8})$$

If the system is in equilibrium, the *time translational invariance* of the previous equation gives the KMS relation:

$$G^{+-}(\omega) \exp(\beta\hbar\omega) = \zeta \exp(\beta\mu) G^{-+}(\omega). \quad (\text{C.9})$$

Using eqs. (B.7) and (B.8), we have on the one hand

$$G^R(\omega) + G^A(\omega) = G^{+-}(\omega)(1 - \zeta \exp(\beta(\hbar\omega - \mu))). \quad (\text{C.10})$$

On the other hand eq. (B.6) implies

$$G^K(\omega) = \frac{i\hbar}{2} G^{+-}(\omega) [1 + \zeta \exp(\beta(\hbar\omega - \mu))]. \quad (\text{C.11})$$

These two last relations yield the grand-canonical quantum FDT:

$$G^K(\omega) = \hbar \tanh \left( \beta \frac{\hbar\omega - \mu}{2} \right)^{-\zeta} \text{Im} G^R(\omega). \quad (\text{C.12})$$

## D Computing the self-energy

### D.1 Derivation within the Schwinger-Keldysh formalism

In the Schwinger-Keldysh path-integral representation we had (see eq. (3.12)) for the whole system (rotors and environment)

$$\mathcal{Z}[\boldsymbol{\eta}^\pm] \equiv \int_{\mathcal{C}} \mathcal{D}[\mathbf{n}^\pm, \boldsymbol{\psi}^\pm, \bar{\boldsymbol{\psi}}^\pm] e^{\frac{i}{\hbar} S[\mathbf{n}^\pm, \boldsymbol{\psi}^\pm, \bar{\boldsymbol{\psi}}^\pm]} \langle \mathbf{n}^+(0), \bar{\boldsymbol{\psi}}^+(0) | \varrho(0) | \mathbf{n}^-(0), \boldsymbol{\psi}^-(0) \rangle, \quad (\text{D.1})$$

At time  $t = 0$ , just after the quench, the initial density is assumed to be factorized:  $\varrho(0) = I_S \otimes \varrho_L^{\text{free}}(0) \otimes \varrho_R^{\text{free}}(0)$  (see Sect. 3.1) yielding

$$\begin{aligned} & \langle \mathbf{n}^+(0), \bar{\boldsymbol{\psi}}^+(0) | \varrho(0) | \mathbf{n}^-(0), \boldsymbol{\psi}^-(0) \rangle \\ &= \delta(\mathbf{n}^+(0) - \mathbf{n}^-(0)) \langle \bar{\boldsymbol{\psi}}_L^+(0) | \varrho_L^{\text{free}}(0) | \boldsymbol{\psi}_L^-(0) \rangle \langle \bar{\boldsymbol{\psi}}_R^+(0) | \varrho_R^{\text{free}}(0) | \boldsymbol{\psi}_R^-(0) \rangle. \end{aligned} \quad (\text{D.2})$$

The generating functional reads

$$\mathcal{Z}[\boldsymbol{\eta}^\pm] = \int_{\mathcal{C}'} \mathcal{D}[\mathbf{n}^+, \mathbf{n}^-] e^{\frac{i}{\hbar} S_S[\mathbf{n}^+, \mathbf{n}^-, \boldsymbol{\eta}]} \langle \langle e^{\frac{i}{\hbar} S_{SB}[\mathbf{n}^+, \boldsymbol{\psi}^+, \bar{\boldsymbol{\psi}}^+, \mathbf{n}^-, \boldsymbol{\psi}^-, \bar{\boldsymbol{\psi}}^-]} \rangle_{\mathcal{L}} \rangle_{\mathcal{R}}. \quad (\text{D.3})$$

The index  $c'$  at the bottom of the integral is here to remind the constraints on the field integration, namely  $\mathbf{n}_i^+(t)^2 = \mathbf{n}_i^-(t)^2 = 1$  and  $\mathbf{n}_i^+(0) = \mathbf{n}_i^-(0) \forall i$ . We introduced the average over the free environment composed of the two reservoirs:

$$\begin{aligned} \langle\langle \cdots \rangle_L \rangle_R &\equiv \int \mathcal{D}[\boldsymbol{\psi}^\pm, \bar{\boldsymbol{\psi}}^\pm] \cdots e^{\frac{i}{\hbar} S_L^L} e^{\frac{i}{\hbar} S_R^R} \\ &\quad \times \langle \bar{\boldsymbol{\psi}}_L^+(0) | \varrho_L^{\text{free}}(0) | \boldsymbol{\psi}_L^-(0) \rangle \langle \bar{\boldsymbol{\psi}}_R^+(0) | \varrho_R^{\text{free}}(0) | \boldsymbol{\psi}_R^-(0) \rangle . \end{aligned} \quad (\text{D.4})$$

We now develop the coupling  $e^{\frac{i}{\hbar} S_{SB}}$  up to the second order,

$$\langle\langle e^{\frac{i}{\hbar} S_{SB}} \rangle_L \rangle_R \simeq 1 + \frac{i}{\hbar} \langle\langle S_{SB} \rangle_L \rangle_R - \frac{1}{2\hbar^2} \langle\langle S_{SB}^2 \rangle_L \rangle_R . \quad (\text{D.5})$$

The first order term is zero. The second order term reads

$$\begin{aligned} \langle\langle S_{SB}^2 \rangle_L \rangle_R &= M \left( \frac{\hbar\omega_c}{N_s} \right)^2 \sum_{ab=\pm} ab \int \int_0^\infty dt dt' \sum_{ij=1}^N \sum_{kk'qq'=1}^{N_s} \sum_{\mu\nu=1}^M \sum_{ll'mm'=1}^{\mathcal{M}} n_i^{\mu a}(t) n_j^{\nu b}(t') \sigma_{ll'}^\mu \sigma_{mm'}^\nu \\ &\quad \times \langle\langle [\bar{\psi}_{Likl}^a(t) \psi_{Rik'l'}^a(t) + L \leftrightarrow R] [\bar{\psi}_{Ljqm}^b(t') \psi_{Rjq'm'}^b(t') + L \leftrightarrow R] \rangle_L \rangle_R . \end{aligned} \quad (\text{D.6})$$

Developing the term on the second line, we obtain

$$\begin{aligned} &\langle\langle [\bar{\psi}_{Likl}^a(t) \psi_{Rik'l'}^a(t) + L \leftrightarrow R] [\bar{\psi}_{Ljqm}^b(t') \psi_{Rjq'm'}^b(t') + L \leftrightarrow R] \rangle_L \rangle_R \\ &= \langle\langle \bar{\psi}_{Rikl}^a(t) \psi_{Lik'l'}^a(t) \bar{\psi}_{Ljqm}^b(t') \psi_{Rjq'm'}^b(t') + L \leftrightarrow R \rangle_L \rangle_R \\ &= -\langle \psi_{Lik'l'}^a(t) \bar{\psi}_{Ljqm}^b(t') \rangle_L \langle \psi_{Rjq'm'}^b(t') \bar{\psi}_{Rikl}^a(t) \rangle_R + L \leftrightarrow R \\ &= \delta_{ij} \delta_{k'q} \delta_{kq'} \delta_{l'm} \delta_{lm'} \hbar^2 [G_{Lk'}^{ab}(t, t') G_{Rk}^{ba}(t', t) + L \leftrightarrow R] . \end{aligned} \quad (\text{D.7})$$

With the free fermionic Green's functions defined on the Keldysh contour as  $i\hbar G_{\alpha k}^{ab}(t, t') = \langle \psi_k^a(t) \bar{\psi}_k^b(t') \rangle_\alpha$  for  $\alpha = L, R$ ,  $a, b = \pm$  and where  $k$  labels the electron's energy. Expression (D.6) now reads

$$\begin{aligned} \langle\langle S_{SB}^2 \rangle_{LR} &= \hbar^2 M \left( \frac{\hbar\omega_c}{N_s} \right)^2 \sum_{ab=\pm} ab \int \int_0^\infty dt dt' \sum_{i=1}^N \sum_{kk'=1}^{N_s} \sum_{\mu\nu=1}^M \sum_{ll'=1}^{\mathcal{M}} n_i^{\mu a}(t) n_i^{\nu b}(t') \sigma_{ll'}^\mu \sigma_{ll'}^\nu \\ &\quad \times [G_{Lk'}^{ab}(t, t') G_{Rk}^{ba}(t', t) + L \leftrightarrow R] . \end{aligned} \quad (\text{D.8})$$

By using the property  $\text{Tr} \sigma^\mu \sigma^\nu = \delta_{\mu\nu}$ , we get

$$\begin{aligned} \langle\langle S_{SB}^2 \rangle_{LR} &= M \hbar^2 \left( \frac{\hbar\omega_c}{N_s} \right)^2 \sum_{ab=\pm} ab \int \int_0^\infty dt dt' \sum_{i=1}^N \mathbf{n}_i^a(t) \cdot \mathbf{n}_i^b(t') \\ &\quad \times \sum_{kk'} [G_{Lk'}^{ab}(t, t') G_{Rk}^{ba}(t', t) + L \leftrightarrow R] . \end{aligned} \quad (\text{D.9})$$

Finally expression (D.5) can be recast into

$$\langle\langle e^{\frac{i}{\hbar} S_{SB}} \rangle_L \rangle_R \simeq e^{\frac{i}{\hbar} S_{SB}^{(2)}} , \quad (\text{D.10})$$

with

$$S_{SB}^{(2)}[\mathbf{n}^+, \mathbf{n}^-] \equiv -\frac{1}{2}M \sum_{ab=\pm} \iint_0^{+\infty} dt dt' \Sigma_B^{ab}(t, t') \sum_{i=1}^N \mathbf{n}_i^a(t) \cdot \mathbf{n}_i^b(t'), \quad (\text{D.11})$$

where the exponent (2) is here to recall that we developed until second order and with the self-energy

$$\Sigma_B^{ab}(t, t') \equiv -abi\hbar (\hbar\omega_c)^2 [G_L^{ab}(t, t')G_R^{ba}(t', t) + G_R^{ab}(t, t')G_L^{ba}(t', t)], \quad (\text{D.12})$$

where the Keldysh Green's functions of the fermions in the  $\alpha$ -reservoir ( $\alpha = L, R$ ) are given by

$$G_\alpha^{ab}(t, t') \equiv \int d\epsilon_\alpha \rho_\alpha(\epsilon_\alpha) G_\alpha^{ab}(\epsilon_\alpha; t - t') = G_\alpha^{ab}(t - t'). \quad (\text{D.13})$$

$\rho_\alpha(\epsilon)$  is the density of states in  $\alpha$ -reservoir and  $G_\alpha^{ab}(\epsilon; \tau)$  are the Keldysh Green's functions of a free fermion with energy  $\epsilon$  in equilibrium in the  $\alpha$ -reservoir (see Appendix B.3.1):

$$\begin{aligned} i\hbar G_\alpha^{+-}(\epsilon; \tau) &= -n_\alpha(\epsilon) e^{-\frac{i}{\hbar}\epsilon\tau}, \\ i\hbar G_\alpha^{-+}(\epsilon; \tau) &= [1 - n_\alpha(\epsilon)] e^{-\frac{i}{\hbar}\epsilon\tau}, \\ i\hbar G_\alpha^{++}(\epsilon; \tau) &= i\hbar G_\alpha^{-+}(\epsilon; \tau)\Theta(\tau) + i\hbar G_\alpha^{+-}(\epsilon; \tau)\Theta(-\tau), \\ i\hbar G_\alpha^{--}(\epsilon; \tau) &= i\hbar G_\alpha^{+-}(\epsilon; \tau)\Theta(\tau) + i\hbar G_\alpha^{-+}(\epsilon; \tau)\Theta(-\tau), \end{aligned} \quad (\text{D.14})$$

with the Fermi factor  $n_\alpha(\epsilon) \equiv (1 + e^{\beta_\alpha(\epsilon - \mu_\alpha)})^{-1}$ . It is clear then that the self-energy is time translational invariant:  $\Sigma_B^{ab}(t, t') \equiv \Sigma_B^{ab}(\tau)$  with  $\tau \equiv t - t'$ . Moreover  $\Sigma_B^{ab}(\tau)$  is a symmetric matrix with respect to time and Keldysh indices:

$$\Sigma_B^{ab}(\tau) = \Sigma_B^{ba}(-\tau), \quad (\text{D.15})$$

Using the time reversal property eq. (A.14) of the Keldysh Green's functions one also establishes

$$\Sigma_B^{ab}(\tau)^* = -\Sigma_B^{\bar{a}\bar{b}}(\tau), \quad (\text{D.16})$$

where we note  $\bar{a} \equiv -a$ .

After a Keldysh rotation of the rotors coordinates, it yields

$$\frac{i}{\hbar} S_{SB}^{(2)}[\mathbf{n}^{(1)}, \mathbf{n}^{(2)}] = \frac{1}{2}M \sum_{rs=(1),(2)} \iint_0^\infty dt dt' \Sigma_B^{rs}(t, t') \sum_{i=1}^N \mathbf{n}_i^r(t) \mathbf{n}_i^s(t'), \quad (\text{D.17})$$

with

$$\begin{aligned} \Sigma_B^{(22)} &= -i\hbar/2 [\Sigma_B^{++} + \Sigma_B^{--}], \\ \Sigma_B^{(21)} &= -i [\Sigma_B^{++} + \Sigma_B^{+-}], \\ \Sigma_B^{(12)} &= -i [\Sigma_B^{++} + \Sigma_B^{-+}], \\ \Sigma_B^{(11)} &= -i/\hbar [\Sigma_B^{++} + \Sigma_B^{+-} + \Sigma_B^{-+} + \Sigma_B^{--}] = 0. \end{aligned} \quad (\text{D.18})$$

which is inverted as

$$i\hbar \Sigma_B^{ab} = -ab \Sigma_B^{(22)} - \frac{\hbar}{2} (a \Sigma_B^{(21)} + b \Sigma_B^{(12)}). \quad (\text{D.19})$$

## D.2 FDT check

We checked that the fermion-reservoir self-energy satisfies the bosonic FDT. This is only valid when the reservoirs constitute an equilibrium bath, *i.e.*,  $\beta_L = \beta_R = \beta$  and  $\mu_L = \mu_R = \mu_0$  ( $V = 0$ ). Note that distribution functions  $\rho_L(\omega)$  and  $\rho_R(\omega)$  can be different although the proof given below uses  $\rho_L(\omega) = \rho_R(\omega) = \rho(\epsilon)$  for simplicity reasons. The goal is to check

$$\Sigma_B^K(\omega) = \hbar \coth\left(\beta \frac{\hbar\omega}{2}\right) \text{Im} \Sigma_B^R(\omega) = \hbar \coth\left(\beta \frac{\hbar\omega}{2}\right) \frac{[\Sigma_B^R + \Sigma_B^A](\omega)}{2i}. \quad (\text{D.20})$$

We first develop the term in the LHS, then we do the same with the RHS to prove their equality.

$$\begin{aligned} \Sigma_B^K(\omega) &= \text{TF} \Sigma_B^K(\tau) \\ &= -2(\hbar\omega_c)^2 \text{TF} \{G^K G^{K*} - \hbar^2/4 [G^A G^{A*} + G^R G^{R*}]\} \\ &= -2(\hbar\omega_c)^2 \text{TF} \{G^K G^{K*} - \hbar^2/4 [G^R + G^A] [G^{R*} + G^{A*}]\}, \end{aligned} \quad (\text{D.21})$$

where we used the nullity of cross terms of the type  $G^R G^A$  since  $G^R \propto \Theta(\tau)$  and  $G^A \propto \Theta(-\tau)$ .

$$\Sigma_B^K(\omega) = -2(\hbar\omega_c)^2 \{G^K \circ G^{K*} - \hbar^2/4 [G^R + G^A] \circ [G^{R*} + G^{A*}]\}, \quad (\text{D.22})$$

where  $\circ$  is the symbol for the convolution (see Appendix A) and  $G^{R*}(\omega)$  stands for the Fourier transform of  $G^R(\tau)^*$ . Since we easily obtain

$$\begin{aligned} G^R(\omega) + G^A(\omega) &= 2i\pi\rho(\hbar\omega), \\ G^{R*}(\omega) + G^{A*}(\omega) &= -2i\pi\rho(-\hbar\omega), \end{aligned} \quad (\text{D.23})$$

and

$$\begin{aligned} G^K(\omega) &= \pi\hbar\rho(\hbar\omega) \tanh\left(\beta \frac{\hbar\omega - \mu_0}{2}\right), \\ G^{K*}(\omega) &= \pi\hbar\rho(-\hbar\omega) \tanh\left(\beta \frac{-\hbar\omega - \mu_0}{2}\right), \end{aligned} \quad (\text{D.24})$$

we get by replacing in (D.22)

$$\begin{aligned} \Sigma_B^K(\omega) &= -2(\hbar\omega_c)^2 (\pi\hbar)^2 \\ &\quad \times \{[\rho(\hbar\omega) \tanh(\beta \frac{\hbar\omega - \mu_0}{2})] \circ [\rho(-\hbar\omega) \tanh(\beta \frac{-\hbar\omega - \mu_0}{2})] - [\rho(\hbar\omega)] \circ [\rho(-\hbar\omega)]\} \\ &= -2(\hbar\omega_c)^2 (\pi\hbar) \int \frac{d\epsilon'}{2\pi} \rho(\epsilon') \rho(\epsilon' - \hbar\omega) \left\{ \tanh\left(\beta \frac{\epsilon' - \mu_0}{2}\right) \tanh\left(\beta \frac{\epsilon' - \hbar\omega - \mu_0}{2}\right) - 1 \right\} \\ &= -\pi\hbar(\hbar\omega_c)^2 \coth\left(\beta \frac{\hbar\omega}{2}\right) \int d\epsilon' \rho(\epsilon') \rho(\epsilon' - \hbar\omega) \left\{ \tanh\left(\beta \frac{\epsilon' - \hbar\omega - \mu_0}{2}\right) - \tanh\left(\beta \frac{\epsilon' - \mu_0}{2}\right) \right\}, \end{aligned} \quad (\text{D.25})$$

where we used the trigonometry relation

$$\tanh(x - y) = \frac{\tanh x - \tanh y}{1 - \tanh x \tanh y}.$$

Let's now calculate the RHS of (D.20).

$$\begin{aligned} \frac{[\Sigma_B^R + \Sigma_B^A](\omega)}{2i} &= i(\hbar\omega_c)^2 \text{TF} \{G^R G^{K*} + G^A G^{K*} + G^K G^{R*} + G^K G^{A*}\} \\ &= i(\hbar\omega_c)^2 \text{TF} \{(G^R + G^A) G^{K*} + G^K (G^{R*} + G^{A*})\} \\ &= i(\hbar\omega_c)^2 \{[G^R + G^A] \circ [G^{K*}] + [G^K] \circ [G^{R*} + G^{A*}]\}, \end{aligned} \quad (\text{D.26})$$

giving

$$\begin{aligned}
& \hbar \coth\left(\beta \frac{\hbar\omega}{2}\right) \frac{[\Sigma_B^R + \Sigma_B^A](\omega)}{2i} \\
&= -2(\pi\hbar)^2 (\hbar\omega_c)^2 \coth\left(\beta \frac{\hbar\omega}{2}\right) \\
&\quad \times \left\{ [\rho(\hbar\omega)] \circ [\rho(-\hbar\omega) \tanh\left(\beta \frac{-\hbar\omega - \mu_0}{2}\right)] - [\rho(\hbar\omega) \tanh\left(\beta \frac{\hbar\omega - \mu_0}{2}\right)] \circ [\rho(-\hbar\omega)] \right\} \\
&= -\pi\hbar (\hbar\omega_c)^2 (2\pi\hbar) \coth\left(\beta \frac{\hbar\omega}{2}\right) \int d\epsilon' \rho(\epsilon') \rho(\epsilon' - \hbar\omega) \left\{ \tanh\left(\beta \frac{\epsilon' - \hbar\omega - \mu_0}{2}\right) - \tanh\left(\beta \frac{\epsilon' - \mu_0}{2}\right) \right\}.
\end{aligned}$$

We recognize here the development (D.25) of  $\Sigma_B^K$ . We just proved that the bosonic FDT is satisfied provided that the two fermionic reservoirs have the same temperature and chemical potential. They can have a different density of states.

## E Dynamics

### E.1 Quadratic effective action

One can render the effective action quadratic at the price of introducing new fields. For a given  $i$  and a given pair of  $(r, \mu, t)$  and  $(s, \nu, t')$ , the identity

$$1 = \int dQ_{i\mu\nu}^{rs}(t, t') \delta\left(n_i^{\mu r}(t) n_i^{\nu s}(t') - Q_{i\mu\nu}^{rs}(t, t')\right), \quad (\text{E.1})$$

becomes, after using the integral representation of the delta distribution (see Appendix A),

$$1 \propto \int dQ_{i\mu\nu}^{rs}(t, t') d\lambda_{i\mu\nu}^{rs}(t, t') \exp\left(-i \frac{M}{2} \lambda_{i\mu\nu}^{rs}(t, t') \left(n_i^{\mu r}(t) n_i^{\nu s}(t') - Q_{i\mu\nu}^{rs}(t, t')\right)\right). \quad (\text{E.2})$$

Introducing similar identities for all possible pairs of  $(r, \mu, t)$  and  $(s, \nu, t')$ , we obtain a path integral over two<sup>3</sup> fields  $Q_{i\mu\nu}^{rs}(t, t')$  and  $\lambda_{i\mu\nu}^{rs}(t, t')$  that are symmetric in the Keldysh indices, times and rotor components:  $Q_{i\nu\mu}^{sr}(t', t) = Q_{i\mu\nu}^{rs}(t, t')$  and  $\lambda_{i\nu\mu}^{sr}(t', t) = \lambda_{i\mu\nu}^{rs}(t, t')$ . The effective action is now also a functional of  $\mathbf{Q}$  and  $\boldsymbol{\lambda}$  and reads

$$\begin{aligned}
\frac{i}{\hbar} S_{\text{eff}} &= -\frac{M}{2} \sum_{r,s=(1),(2)} \iint dt dt' \sum_i \sum_{\mu\nu} n_i^{\mu r}(t) [Op_{i\mu\nu}^{rs}(t, t') + i\lambda_{i\mu\nu}^{rs}(t, t')] n_i^{\nu s}(t') \\
&+ \frac{J^2 M^2}{2N} \sum_{i,j} \iint dt dt' \sum_{\mu,\nu} Q_{i\mu\nu}^{(11)}(t, t') Q_{j\mu\nu}^{(22)}(t, t') + Q_{i\mu\nu}^{(12)}(t, t') Q_{j\mu\nu}^{(21)}(t, t') \\
&+ \frac{i}{\hbar} \frac{M}{2} \sum_a a \int dt \sum_i z_i^a(t) + i \frac{M}{2} \sum_{rs} \iint dt dt' \sum_i \sum_{\mu\nu} \lambda_{i\mu\nu}^{rs}(t, t') Q_{i\mu\nu}^{rs}(t, t') \\
&+ \text{boundary terms},
\end{aligned} \quad (\text{E.3})$$

---

<sup>3</sup>There are  $N(M^2 K^2 + MK)/2$  of each of these fields, where  $K = 2$  is the number of possible Keldysh indices.



where we introduced the operator  $Op_{i\mu\nu}^{rs}(t, t')$  defined as

$$\begin{aligned}
Op_{i\mu\nu}^{(12)}(t, t') &\equiv i\delta_{\mu\nu}\delta(t-t') \left[ \frac{1}{\Gamma}\partial_{t'}^2 + \frac{1}{2}\sum_{a=\pm} z_i^a(t) \right] - i\delta_{\mu\nu}\Sigma_B^R(t', t), \\
Op_{i\mu\nu}^{(21)}(t, t') &\equiv Op_{i\nu\mu}^{(12)}(t', t), \\
Op_{i\mu\nu}^{(22)}(t, t') &\equiv \frac{i\hbar}{4}\delta_{\mu\nu}\delta(t-t') \sum_{a=\pm} az_i^a(t) + \delta_{\mu\nu}\Sigma_B^K(t, t'), \\
Op_{i\mu\nu}^{(11)}(t, t') &\equiv \frac{i}{2\hbar}\delta_{\mu\nu}\delta(t-t') \sum_{a=\pm} az_i^a(t).
\end{aligned} \tag{E.4}$$

$Op_{i\mu\nu}^{rs}(t, t')$  is symmetric in the Keldysh indices, times and rotor components:  $Op_{i\nu\mu}^{sr}(t', t) = Op_{i\mu\nu}^{rs}(t, t')$ . The functional integration over  $n_i^{\mu r}$  is now quadratic and can be performed, leading to

$$\begin{aligned}
\frac{i}{\hbar}S_{\text{eff}} &= -\frac{1}{2}\text{Tr} \ln M (Op + i\lambda) \\
&\quad - \frac{J^2 M^2}{2N} \sum_{i,j} \iint dt dt' \sum_{\mu,\nu} Q_{i\mu\nu}^{(11)}(t, t') Q_{j\mu\nu}^{(22)}(t, t') + Q_{i\mu\nu}^{(12)}(t, t') Q_{j\mu\nu}^{(21)}(t, t') \\
&\quad + \frac{i}{\hbar} \frac{M}{2} \sum_a a \int dt \sum_i z_i^a(t) + i \frac{M}{2} \sum_{rs} \iint dt dt' \sum_i \sum_{\mu\nu} \lambda_{i\mu\nu}^{rs}(t, t') Q_{i\mu\nu}^{rs}(t, t')
\end{aligned} \tag{E.5}$$

where the trace in the first term is spanning the whole space of indices, namely rotor sites, Keldysh indices, times and rotor components.

## E.2 Saddle-point evaluation

In this subsection, we evaluate in the limit  $M \rightarrow \infty$  the saddle-point equations with respect to the dummy fields we introduced previously, namely  $\lambda_{i\mu\nu}^{rs}(t, t')$ ,  $Q_{i\mu\nu}^{rs}(t, t')$  and  $z_i^a(t)$ . The fluctuations around the saddle are neglected. In particular, using eq. (E.1) we have the identity (see the definition of Green's functions in Sect. 3.3.4)

$$Q_{i\mu\nu}^{rs}(t, t') = i\hbar G_{ii\mu\nu}^{rs}(t, t'). \tag{E.6}$$

Along the lines we prove that the solution in the saddle is  $O(NM)$ , like the starting Hamiltonian.

The saddle-point with respect to  $\lambda_{i\mu\nu}^{rs}(t, t')$  yields

$$\frac{\delta S_{\text{eff}}}{\delta \lambda_{i\mu\nu}^{rs}(t, t')} = -\frac{1}{2} \text{Tr} \frac{\delta}{\delta \lambda_{i\mu\nu}^{rs}(t, t')} \ln M (Op + i\lambda) + i \frac{M}{2} Q_{i\mu\nu}^{rs}(t, t') = 0, \tag{E.7}$$

giving in matrix notations

$${}^t(Op + i\lambda)^{-1} = MQ, \tag{E.8}$$

where the symbol  ${}^t$  represents the transposition. Since all operators in the last equation are symmetric by definition, we get

$$Op + i\lambda = \frac{1}{M} Q^{-1}. \tag{E.9}$$

The saddle-point equation with respect to  $Q_{i\mu\nu}^{rs}(t, t')$  yields

$$i\lambda_{i\mu\nu}^{rs}(t, t') = \frac{J^2 M}{N} \sum_j Q_{j\mu\nu}^{\bar{r}\bar{s}}(t, t') \quad \forall i, \quad (\text{E.10})$$

where  $\overline{(2)} \equiv (1)$  and  $\overline{(1)} \equiv (2)$ . The RHS of this last equation being site-independent,  $\lambda_{i\mu\nu}^{rs}(t, t')$  does not depend on  $i$ :  $\lambda_{i\mu\nu}^{rs}(t, t') = \lambda_{\mu\nu}^{rs}(t, t')$ . Equations (E.9) and (E.10) imply

$$Op_i^{rs} + \frac{J^2 M}{N} \sum_j Q_j^{\bar{r}\bar{s}} - \frac{1}{M} Q^{-1}{}^i{}^{rs} = 0. \quad (\text{E.11})$$

The saddle-point equation with respect to  $z_i^a(t)$  yields to the two equations:

$$\begin{aligned} \sum_{\mu} ([Op + i\lambda]^{-1})_{i\mu\mu}^{(12)}(t, t) + ([Op + i\lambda]^{-1})_{i\mu\mu}^{(21)}(t, t) &= 0, \\ \sum_{\mu} ([Op + i\lambda]^{-1})_{i\mu\mu}^{(11)}(t, t) + \frac{\hbar^2}{4} ([Op + i\lambda]^{-1})_{i\mu\mu}^{(22)}(t, t) &= M. \end{aligned} \quad (\text{E.12})$$

This is nothing more than the constraint that rotors should have a unit length. However,  $\lambda$  being site-independent, it is clear from these equations that it has to be the same for  $Op$ . Finally at the saddle,  $Op$ ,  $Q$  and  $z$  are site-independent (homogeneous) so we can get rid of the sites indices:  $Op_{i\mu\nu}^{rs}(t, t') = Op_{\mu\nu}^{rs}(t, t')$ ,  $Q_{i\mu\nu}^{rs}(t, t') = Q_{\mu\nu}^{rs}(t, t')$  and  $z_i^a(t) = z^a(t)$ . Equation (E.11) becomes

$$Op^{rs} + J^2 M Q^{\bar{r}\bar{s}} - \frac{1}{M} Q^{-1rs} = 0. \quad (\text{E.13})$$

Since from its definition (E.4)  $Op_{\mu\nu}^{rs}(t, t') \propto \delta_{\mu\nu}$ , the previous equation tells us that it has to be the same for  $Q_{\mu\nu}^{rs}(t, t')$  so we can get rid of all the rotor component indices. Multiplying by  $Q^{sv}(t', t'')$ , and summing over  $s$  and  $t'$ , we get

$$\int dt' \sum_s Op^{rs}(t, t') Q^{sv}(t', t'') + J^2 M Q^{\bar{r}\bar{s}}(t, t') Q^{sv}(t', t'') - \frac{1}{M} \delta_{rv} \delta(t - t'') = 0. \quad (\text{E.14})$$

The macroscopic Green's function reading  $i\hbar G^{rs}(t, t') = M Q^{rs}(t, t')$  we obtain

$$\int dt' \sum_s Op^{rs}(t, t') i\hbar G^{sv}(t', t'') + J^2 i\hbar G^{\bar{r}\bar{s}}(t, t') i\hbar G^{sv}(t', t'') - \delta_{rv} \delta(t - t'') = 0. \quad (\text{E.15})$$

### E.3 Schwinger-Dyson equations

The  $(r = (2), v = (1))$  component of eq. (E.15) gives a complex equation the real part of which yields

$$z^+(t) = z^-(t) \equiv z(t) \quad \forall t, \quad (\text{E.16})$$

and the imaginary part of which is the dynamic equation for the self-correlation:

$$\left[ \frac{1}{\Gamma} \frac{\partial^2}{\partial t^2} + z(t) \right] C(t, t') = \int_0^{t'} dt'' \Sigma^K(t, t'') R(t', t'') + \int_0^t dt'' \Sigma^R(t, t'') C(t'', t'), \quad (\text{E.17})$$

where we introduced

$$\Sigma^K \equiv J^2 C + \Sigma_B^K, \quad \Sigma^R \equiv J^2 R + \Sigma_B^R. \quad (\text{E.18})$$

Similarly, the  $(r = (2), v = (2))$  component of eq. (E.15) yields the equation of motion for the self-response:

$$\left[ \frac{1}{\Gamma} \frac{\partial^2}{\partial t^2} + z(t) \right] R(t, t') = \delta(t - t') + \int_{t'}^t dt'' \Sigma^R(t, t'') R(t'', t'). \quad (\text{E.19})$$

The  $(r = (1), v = (1))$  component of eq. (E.15) leads to the same equation and the  $(r = (1), v = (2))$  component expresses  $0 = 0$ . Setting  $t' = t$  in eq. (E.17) we obtain the expression for the Lagrange multiplier

$$z(t) = \int_0^t dt'' \Sigma^K(t, t'') R(t, t'') + \Sigma^R(t, t'') C(t, t'') - \frac{1}{\Gamma} \frac{\partial^2 C}{\partial t^2}(t, t' \rightarrow t^-). \quad (\text{E.20})$$

Equations (E.17) and (E.19) together with eq. (E.20) constitute the Schwinger-Dyson equations that fully determine the dynamics of the interacting system.

## References

- [1] A. J. Leggett, S. Chakravarty, A. T. Dorsey, M. P. A. Fisher, A. Garg, W. Zwerger, *Rev. Mod. Phys.* **59**, 1 (1987).
- [2] I.S. Tupitsyn and B. Barbara, *Quantum tunneling of magnetization in molecular complexes with large spins. Effect of the environment*. Magnetism: Molecules to Materials III, 109 (Wiley, New York, 2001).
- [3] See *e.g.* P. Calabrese and J. Cardy, *J. Phys. A* **42**, 504005 (2009).
- [4] D. Segal, D. R. Reichman and A. J. Millis, *Phys. Rev. B* **76**, 195316 (2007).
- [5] S. Miyashita, S. Tanaka, H. De Raedt, and B. Barbara, *J. Phys.: Conf. Ser.* **143** 012005 (2009).
- [6] T. Kadowaki and H. Nishimori, *Phys. Rev. E* **58**, 5355 (1998).  
E. Farhi, J. Goldstone, S. Gutmann, J. Lapan, A. Lundgren, and D. Preda, *Science* **292**, 472 (2001).  
G. E. Santoro and E. Tosatti, *J. Phys. A* **39**, R393 (2006).
- [7] A. Polkovnikov, *Phys. Rev. B* **72**, 161201 (2005).  
W. H. Zurek, U. Dorner, and P. Zoller, *Phys. Rev. Lett.* **95**, 105701 (2005).
- [8] L. F. Cugliandolo, G. S. Lozano, and H. Lozza, *Phys. Rev. B* **71**, 224421 (2005).  
G. Schehr and H. Rieger *Phys. Rev. Lett.* **96**, 227201 (2006). *J. Stat. Mech.* (2008) P04012.

- [9] L. Arrachea, Phys. Rev. B **70**, 155407 (2004).  
A. Caso, L. Arrachea, and G. S. Lozano, Phys. Rev. B **81**, 041301 (2010)
- [10] L. Arrachea and L. F. Cugliandolo Europhys. Lett. **70**, 642 (2005).
- [11] A. Onuki and K. Kawasaki, Ann. Phys. (N. Y.) **121**, 456 (1979).
- [12] H. Hinrichsen, Adv. Phys. **49** 815 (2000).
- [13] B. Schmittmann and R. K. P. Zia, Vol. 17 of Phase Transitions and Critical Phenomena, eds. C. Domb and J. L. Lebowitz (Academic Press, London, 1995).
- [14] U. C. Täuber, Chap. 7 of Ageing and the Glass Transition in Lecture Notes in Physics (Springer, Berlin, 2007).
- [15] L. C. E. Struick, *Physical Aging in Amorphous Polymers and Other Materials*, (Elsevier, Amsterdam, 1978).
- [16] L. F. Cugliandolo, in Les Houches Session LXXVII, J-L. Barrat *et al* eds. (Springer-EDP Sciences, Berlin-Les Ulis, 2003).
- [17] D. Dalidovich and P. Phillips, Phys. Rev. Lett. **93**, 027004 (2004).
- [18] A. G. Green and S. L. Sondhi, Phys. Rev. Lett. **95**, 267001 (2005).
- [19] P. M. Hogan and A. G. Green, arXiv:cond-mat/0607522.
- [20] A. Mitra, S. Takei, Y. B. Kim, and A. J. Millis, Phys. Rev. Lett. **97**, 236808 (2006).
- [21] D. E. Feldman, Phys. Rev. Lett. **95**, 177201 (2005).
- [22] A. Mitra and A. J. Millis, Phys. Rev. B **77**, 220404 (2008).
- [23] C. Aron, G. Biroli, and L. F. Cugliandolo, Phys. Rev. Lett. **102**, 050404 (2009).
- [24] S. Sachdev, *Quantum Phase Transitions*, (Cambridge Univ. Press, 1999).
- [25] U. Weiss, *Quantum dissipative systems* (World Scientific, Singapore, 1993).
- [26] A. Kamenev, arXiv:cond-mat/0412296, arXiv:cond-mat/0109316.
- [27] J. Ye, S. Sachdev, and N. Read, Phys. Rev. Lett. **70**, 4011 (1993).  
T. K. Kopec, Phys. Rev. B **50**, 9963 (1994).
- [28] P. Shukla and S. Singh, Phys. Lett. A **81**, 477 (1981).
- [29] M. Rokni and P. Chandra, Phys. Rev. B **69**, 094403 (2004).
- [30] L. F. Cugliandolo and D. S. Dean, J. Phys. A **28**, 4213 (1995).  
L. F. Cugliandolo and D. S. Dean, J. Phys. A **28**, L453 (1995).

- [31] L. F. Cugliandolo and G. S. Lozano, Phys. Rev. B **59**, 915 (1999).  
L. F. Cugliandolo and G. S. Lozano, Phys. Rev. Lett. **80**, 4979 (1998).
- [32] A. Schmid, J. Low Temp. **49**, 609 (1982).  
A. O. Caldeira and A. J. Leggett, Physica A **121**, 587 (1983).  
H. Grabert, P. Schramm and G.-L. Ingold, Phys. Rep. **168**, 115 (1988).  
C. Greiner and S. Leupold, Ann. Phys. **270**, 328 (1998).
- [33] A. S. Núñez and R. A. Duine, Phys. Rev. B **77**, 054401 (2008).
- [34] D. M. Basko and M.G. Vavilov, Phys. Rev. B **79**, 064418 (2009).
- [35] L. F. Cugliandolo, D. R. Grempel, G. S. Lozano, H. Lozza, and C. A. da Silva Santos, Phys. Rev. B **66**, 014444 (2002).  
L. F. Cugliandolo, D. R. Grempel, G. S. Lozano, and H. Lozza, Phys. Rev. B **70**, 024422 (2004).
- [36] L. F. Cugliandolo, J. Kurchan, and L. Peliti, Phys. Rev. E **55**, 3898 (1997).
- [37] M. P. Kennett and C. Chamon, Phys. Rev. Lett. **86**, 1622 (2001).  
M. P. Kennett, C. Chamon, and J. Ye, Phys. Rev. B **64**, 224408 (2001).  
G. Biroli and O. Parcollet, Phys. Rev. B **65**, 094414 (2002).  
H. Westfahl, J. Schmalian, P. G. Wolynes, Phys. Rev. B **68**, 134203 (2003). G. Busiello, E. V. Gazeeva, R. V. Saburova, I. R. Khaibutdinova, G. P. Chugunova, Physics of metals and metallography **97**, 552 (2004); *ibid* **101**, 109 (2006); *ibid* **102**, 244 (2006). L. F. Cugliandolo, T. Giamarchi, and P. Le Doussal, Phys. Rev. Lett. **96**, 217203 (2006).
- [38] R. Kubo, M. Toda, and N. Hashitsume, *Statistical physics II: Nonequilibrium stastical mechanics*, (Springer, New York 1985).
- [39] J. Zinn-Justin, *Quantum Field Theory and Critical Phenomena* (Oxford Univ. Press, 2002).
- [40] G. Biroli and L. F. Cugliandolo, Phys. Rev. B **64**, 014206 (2001).
- [41] See, for example, D. Goldhaber-Gordon et al., Nature (London) **391**, 156 (1998).  
D. Goldhaber-Gordon et al., Phys. Rev. Lett. **81**, 5225 (1998).  
W. Liang et al., Nature (London) **417**, 725 (2002).
- [42] P. Mehta and N. Andrei, Phys. Rev. Lett. **96**, 216802 (2006).  
S. Kehrein, Phys. Rev. Lett. **95**, 056602 (2005).  
E. Boulat, H. Saleur, and P. Schmitteckert, Phys. Rev. Lett. **101**, 140601 (2008).  
B. Doyon, N. Andrei, Phys. Rev. B **73**, 245326 (2006).
- [43] R. Landauer, IBM, J. Res. Dev. **1**, 223 (1957); Philos. Mag. **21**, 863 (1970).  
M. Büttiker, Phys. Rev. Lett. **57**, 1761 (1986).